C21

Synaptic activation of kainate receptors inhibits I_{sAHP} in CA1 pyramidal neurones

Z. Melyan, B. Lancaster* and H.V. Wheal

*Neurosciences Group, University of Southampton, Southampton SO16 7PX, UK and *Wolfson Institute for Biomedical Research, University College London, London WC1E 6BT, UK*

In CA1 pyramidal neurones a slow afterhyperpolarisation current (I_{sAHP}) regulates action potential firing frequency. Exogenous kainate application (10–100 nM) inhibits I_{sAHP} leading to an increase in excitability. This effect is mediated by a metabotropic action of postsynaptic kainate receptors (KARs), presumably containing GluR6 subunits, on CA1 pyramidal cells (Melyan *et al.* 2002). We investigated whether synaptic activation of these receptors can evoke inhibition of I_{sAHP} similar to that produced by kainate application.

Hippocampal slices were obtained from humanely killed 14- to 21-day-old rats. Whole-cell recordings using $KMeSO_4$-based solution were made from CA1 pyramidal cells. Voltage steps (60 mV for 80 ms) were applied every 20 s to generate I_{sAHP}. The effect of synaptically released glutamate was assessed by comparing I_{sAHPs} induced before and after a train of stimuli delivered via a stimulating electrode (Heuss *et al.* 1999). Data are expressed as means ± S.E.M.

Trains of synaptic stimuli (5 pulses, 100 Hz) previously shown to activate KARs (Min *et al.* 1999) produced 33 ± 1 % inhibition of I_{sAHP} amplitude ($n = 8$). In order to isolate KAR responses, experiments were carried out in the presence of a cocktail of antagonists to block NMDAR (100 μM DL-AP5), AMPAR (100 μM GYKI52466), mGluR (1 mM MCPG and 250 μM MSOP), $GABA_AR$ (100 μM picrotoxin), $GABA_BR$ (200 μM 2-OH-saclofen), muscarinic AChR (1 μM atropine sulphate), opioid (10 μM naloxone), cannabinoid CB_1 (2 μM AM 251) and adenosine receptors (0.1 μM DPCPX). The I_{sAHP} inhibition was not reversible within 30 min, similar to observations with kainate application. The I_{sAHP} inhibition was effectively blocked by prior application of 20 μM CNQX ($n = 6$) confirming that it was mediated by kainate receptor activation. The glutamate uptake blocker TBOA (50–100 μM) increased the effect of synaptic stimulation on I_{sAHP} to 50 ± 2 % inhibition ($n = 8$). Increasing the number of stimuli to 10 or 20 also increased I_{sAHP} inhibition to 38 ± 7 % ($n = 4$) and 54 ± 2 % ($n = 4$), respectively, whereas a single stimulus had no effect ($n = 3$).

We conclude that synaptically released glutamate acting on kainate receptors can reduce I_{sAHP} in CA1 pyramidal neurons indicating a direct role for kainate receptors in regulation of CA1 pyramidal cell excitability.

Heuss C *et al.* (1999). *Nat Neurosci* **2**, 1070–1077.

Melyan Z *et al.* (2002). *Neuron* **34**, 107–114.

Min MY *et al.* (1999). *Proc Natl Acad Sci USA* **96**, 9932–9937.

The work is supported by The Wellcome Trust.

All procedures accord with current UK legislation.

C22

Potassium channel modulation following cyclic AMP elevation in hippocampal neurones

B. Lancaster†, H. Hu* and J.F. Storm*

*†Wolfson Institute for Biomedical Research, University College London, Gower Street, London WC1E 6BT, UK and *Institute of Physiology, University of Oslo, PB 1103 Blindern, 0317 Oslo, Norway*

Modulation of ion channels by metabotropic transmitters and receptors is a widespread mechanism for the regulation of excitability in the brain. These mechanisms are slow compared with ionotropic receptors but the speed of modulation is difficult to discern independently of the agonist–receptor interaction in intact tissue. We used photolysis of caged cAMP to reveal the time course of the cAMP-dependent modulation of the Ca^{2+}-dependent K^+ current I_{sAHP} in hippocampal neurones.

Hippocampal slices were obtained from humanely killed 16- to 21-day-old rats. Whole-cell recordings were made from CA1 pyramidal cells using $KMeSO_4$-based solutions plus DMNB-caged cAMP. Prolonged photolysis of caged cAMP was produced by a xenon lamp and UV filter on an upright microscope. Rapid photolysis was achieved with a flashlamp. I_{sAHP} was evoked either by depolarising voltage steps or internal perfusion with 1 mM dibromo-BAPTA (DBB, Lancaster & Batchelor, 2000) to produce a persistently active I_{sAHP}. Data are expressed as means ± S.E.M. sAHP charge was measured as 1 s integrals of the current commencing 500 ms from the end of the depolarising step.

Flash photolysis of 200 μM caged cAMP (1 ms flash discharge) caused almost complete inhibition of depolarization-evoked I_{sAHP} (94 ± 9 %, $n = 4$). In contrast, prolonged photolysis (30 s UV) of 200 μM caged cAMP was less effective and inhibited I_{sAHP} by 56 ± 10 % ($n = 4$). Similar prolonged photolysis with the persistently active I_{sAHP} showed that inhibition became evident 2–3 s after the onset of UV exposure and reached a steady state of 43 ± 5 % ($n = 5$) after 20 s. The sAHP charge was also inhibited by bath application of the phosphodiesterase (PDE) inhibitor IBMX (1 mM; 105 ± 27 to 23 ± 12 pC, $n = 5$). This is consistent with tonic PDE activity which restrains accumulation of cAMP. Further definition of the onset of inhibition was obtained using a flashlamp linked to a 700 μm fibre-optic bundle. The fibre-optic tip was placed through the solution interface adjacent to the tissue, so minimising inter-experiment variability. Photolysis of increasing concentrations of caged cAMP (40, 200 and 1000 μM; $n = 5$ in each case) caused progressively greater and more rapid inhibition of the K^+ current with time constants of 4229 ± 638 ms (40 μM), 2213 ± 183 ms (200 μM) and 1650 ± 186 ms (1000 μM).

These data indicate some of the temporal limits of cAMP-dependent regulation of neuronal ion channels.

Lancaster B & Batchelor AM (2000). *J Physiol* **522**, 231–246.

This work was supported by The Wellcome Trust, Sir Jules Thorn Charitable Trust and Norwegian Research Council.

All procedures accord with current UK legislation.

C23

Regulation of excitability in cholinergic basal forebrain neurones by K_{ATP} channels

T.G.J. Allen

Department of Pharmacology, University College London, Gower Street, London WC1E 6BT, UK

Brain slice and dissociated cell culture preparations were used to investigate the role of K_{ATP} channels in controlling the excitability of cholinergic neurones from the medial septum, diagonal band and substantia innominata of 12- to 14-day-old rats. Animals were anaesthetised by chloroform inhalation before being killed according to Home Office guidelines.

In the absence of ATP in the pipette filling solution cell excitability fell markedly within the first few minutes of establishing whole-cell conditions. Typically, cell membrane potential hyperpolarised by 13.4 ± 1.6 mV ($n = 24$), whilst resting membrane conductance increased by 13.2 ± 1.7 nS ($n = 24$). This resulted in a 5- to 10-fold increase in the stimulating current required to evoke action potential discharge. These effects could be reversed by exposure to the sulphonylurea compounds glibenclamide (10 nM) or tolbutamide (100 μM). However, inclusion of MgATP (0.1–4 mM), in the pipette solution failed to prevent activation of the underlying conductance.

Under voltage clamp, the sulphonylurea-sensitive current had an almost linear *I/V* relationship between −120 and −40 mV, exhibited no time dependence and reversed close to E_K. Changes in $[K^+]_o$ shifted the reversal potential by 59.6 mV for a 10-fold increase in $[K^+]_o$ ($n = 5$).

Simultaneous whole-cell and cell-attached patch recording with 118 mM K^+-containing solution in both electrodes and 3 mM K^+ in the bath solution, revealed that the current was associated with the opening of channels of conductance of 60–74.5 pS (mean ± S.E.M. 66.2 ± 1.9 pS, $n = 7$). Both the current and channel activity were inhibited reversibly by tolbutamide (100 μM) and irreversibly by glibenclamide (10 nM). In inside-out patches recorded in symmetrical 140 mM K^+-containing solution (potassium acetate 140 mM, Hepes 20 mM, $MgCl_2$ 1 mM, EGTA 1 mM; pH 7.3) the K_{ATP} channels exhibited weak inward rectification at positive membrane potentials. Channel opening was reversibly inhibited by 10 μM MgATP. In the presence of 100 μM MgATP, ADP and diazoxide but not pinacidil (200 μM) increased channel opening.

These data indicate that K_{ATP} channels exert a profound modulatory influence upon the excitability of cholinergic basal forebrain neurones. Single-channel conductance and pharmacological data are consistent with them being composed of SUR1 and Kir 6.2 subunits. Furthermore, whilst they show a high affinity for inhibition by ATP in excised patches, in the intact cell their sensitivity to ATP is more than two orders of magnitude lower, indicating that the channels are under tonic modulation by factors such as PIP_2 (Baukrowitz *et al.* 1998) that are washed out or lost following excision.

Baukrowitz T *et al.* (1998). *Science* **282**, 1141–1144.

This work is supported by the MRC.

All procedures accord with current UK legislation.

C24

Coupling of P2Y nucleotide receptors to G-protein-gated inward rectifying K^+ channels

A.K. Filippov*, J.M. Fernandez-Fernandez†, E.A. Barnard‡ and D.A. Brown*

**Department of Pharmacology, University College London, Gower Street, London WC1E 6BT, †Department of Experimental Sciences and Health, Pompeu Fabra University, 08003 Barcelona, Spain and ‡Department of Pharmacology, University of Cambridge, Tennis Court Road, Cambridge CB2 1QJ, UK*

Cloned G-protein-coupled nucleotide $P2Y_1$, $P2Y_2$, $P2Y_4$ and $P2Y_6$ receptors mediate inhibition of neuronal Ca^{2+} and M-type K^+ currents when expressed in rat superior cervical sympathetic (SCG) neurones (Brown *et al.* 2000). The recently cloned $P2Y_{12}$ receptor also produces stable activation of G-protein-gated inward rectifier K^+ (GIRK) current (Simon *et al.* 2002). We report here that $P2Y_1$, $P2Y_4$ and $P2Y_6$ receptors also modulate GIRK currents when expressed in SCG neurones.

cDNA for individual P2Y receptors was co-injected with cDNA for GIRK1 and GIRK2 channels into the nucleus of cultured SCG neurones (isolated from rats killed by approved Schedule 1 methods). After overnight incubation cells expressed both receptors and functional GIRK channels. Currents were recorded using either perforated-patch or whole-cell (disrupted patch) techniques, with similar results.

Stimulation of $P2Y_1$ receptors with 2-MeSADP (1 μM) induced activation of GIRK current followed by inhibition ($n = 15$). In contrast, stimulation of endogenous α_2-adrenoceptors by noradrenaline produced stable activation without inhibition. $P2Y_1$-mediated inhibition was also seen when 2-MeSADP was applied after GIRK current preactivation by noradrenaline or expression of $G\beta_1\gamma_2$ subunits ($n = 10$).

Stimulation of $P2Y_4$ receptors with UTP (100 μM) ($n = 13$) or $P2Y_6$ receptors with UDP (10 μM) ($n = 15$) only weakly activated GIRK current but significantly inhibited preactivated current.

Current activation by $P2Y_1$ receptors was prevented by overnight pretreatment with Pertussis toxin (PTX), whereas inhibition of GIRK current by all three nucleotide receptors was insensitive to PTX. Inhibition of the GIRK current was not affected after co-expression of RGS11 ($n = 3$) that interferes with $G_q\beta\gamma$ pathway or after co-expression of PLCδ-PH ($n = 5$), a construct that sequesters the membrane phospholipid $PI(4,5)P_2$. In contrast, inhibition was significantly reduced after co-expression of RGS2 protein ($n = 9$), which is known to inhibit $G_q\alpha$ signalling. Buffering of intracellular Ca^{2+} after 1–4 h pre-incubation with BAPTA-AM (10 μM) ($n = 2$), or pre-treatment with protein kinase C inhibitor, GF 109203X (1 μM) ($n = 5$), did not change GIRK current inhibition.

We conclude that activation of GIRK current by cloned P2Y receptors can be related to $G_{i/o}\beta\gamma$ while inhibition – to $G_q\alpha$. These effects may provide a mechanism for the modulation of excitability in the brain by P2Y receptors.

Brown DA *et al.* (2000). *J Aut Nerv Syst* **81**, 31–36.

Simon J *et al.* (2002). *J Biol Chem* **277**, 31390–31400.

This work was supported by The Wellcome Trust.

All procedures accord with current UK legislation.

C25

Kv1 conductances regulating principal neurone excitability in the rat LSO follow the tonotopic axis

Margaret Barnes-Davies, Fatima Osmani, Matthew C. Barker and Ian D. Forsythe

Department of Cell Physiology and Pharmacology, University of Leicester, PO Box 138, Leicester LE1 9HN, UK

The lateral superior olive (LSO) is a binaural brainstem nucleus, involved in sound source localisation. Principal LSO neurones are excited by tones applied to the ipsilateral ear, inhibited by contralateral tones and show a mediolateral tonotopic gradient (high to low frequencies). Their action potential (AP) firing response to tone bursts is described as a 'chopper' pattern in post-stimulus time histograms. Dendrotoxin (DTX)-sensitive low-threshold K^+ currents (I_{LT}) mediated by Kv1 channels are important in regulating AP firing in other auditory neurones (Dodson *et al.* 2002). We used whole-cell voltage and current clamp recording in rat brainstem slices to study low-threshold currents underlying LSO principal neurone firing.

Lister Hooded rats (8–14 days old) were killed by decapitation and 150 μm transverse brainstem slices prepared. Slices were superfused with normal ACSF, bubbled with 5 % CO_2 and 95 % O_2 at 25 °C and LSO neurones whole-cell patch clamped with pipettes containing a 130 mM KCl-based patch solution and 1 mg ml^{-1} Lucifer Yellow. Data are means ± S.E.M.

Principal neurones had sustained outward currents in response to depolarising commands and a slowly developing inward current in response to hyperpolarizing commands. The inward current was blocked by 10 μM ZD7288, confirming that it was the non-selective cation current I_h. Principal neurones had a spectrum of AP firing patterns in response to depolarising current injection. Some cells fired a single 'onset' AP whilst others had an accommodating train following the precisely timed initial AP, described as a 'chopper' response (Adam *et al.* 1999). *I–V* relationships revealed that 'onset' cells had more outward current at −40 mV, suggesting I_{LT} may regulate their firing. Current density at −40 mV was 0.039 ± 0.003 nA pF^{-1}; $n = 10$ compared with 0.016 ± 0.002 nA pF^{-1}; $n = 11$ in 'chopper' cells ($P < 0.001$; unpaired t test). Application of 100 nM DTX-I reduced the outward current at −40 mV by 94 ± 3 % ($n = 5$) in 'onset' neurones and converted the single 'onset' AP into a 'chopper'-like train, confirming the presence of Kv1 conductances.

Plotting the location of each principal neurone on a stereotypical LSO profile showed that 'onset' cells dominated in the low frequency lateral limb and 'chopper' cells in the high frequency medial limb. Immunohistochemical localisation of Kv1.1 subunits in three rats showed a mediolateral intensity gradient with highest levels in the lateral LSO. We conclude that LSO principal cells display a range of AP firing patterns which are tonotopically distributed and Kv1 regulated.

Adam TJ *et al.* (1999). *Exp Brain Res* **124**, 489–502.

Dodson PD *et al.* (2002). *J Neurosci* **22**, 6953–6961.

This work was supported by The Wellcome Trust and The Physiological Society.

All procedures accord with current UK legislation.

C26

Action potential invasion of axon collaterals of rat hippocampal CA1 pyramidal cells has a high safety factor

S. Baudoux and C.D. Richards

Department of Physiology, University College London, Gower Street, London WC1E 6BT, UK

In the CNS, action potentials are propagated through complex axonal arbours. It has been suggested that this process is subject to failure at axon branch points (Bielefeldt & Jackson, 1993; Debanne *et al.* 1997), although this has been disputed by others (Cox *et al.* 2000). Here we report some experiments showing that action potentials reliably invade axon collaterals of hippocampal CA1 neurons.

Eight-day-old rat pups were killed by cervical dislocation and hippocampal slices (250 μm thick) prepared and cultured as described by Stoppini *et al.* (1991) for 7–14 days before use. Whole-cell patch-clamp recordings were made from CA1 pyramidal cells. The pipette filling solution contained the calcium indicator 200 μM Oregon Green BAPTA-1. Once a cell had been successfully patched, it was imaged using two photon microscopy and the axon traced until a branch point was found. Thereafter, line scans were used to record the calcium transients elicited by action potentials triggered by depolarising the cell body. The presence of a calcium transient was taken as evidence of action potential invasion of the axon under investigation.

Calcium transients were recorded both from the main axon and axon collaterals at distances between 45 and 230 μm from the cell body. Following stimulation, the calcium concentration in the axon rose from baseline to peak within 2–4 ms. The fractional change in basal fluorescence ($\Delta F/F$) was 0.41 ± 0.04 ($n = 30$; S.E.M.). We subsequently recorded evoked calcium transients from 15 main axons and their collaterals after clearly identified branch points. In no case did the action potential fail to invade the main axon or the collateral branch ($n = 77$ trials). Invasion of the axonal arbour was also reliable during short trains of action potentials (20–100 Hz). To estimate the safety factor for action potential invasion of collaterals, we recorded from eleven axon branches in the presence of lidocaine (120–250 μM) or procaine (500 μM) that reduced the inward current by 20–30 %. In all cases, the action potential successfully invaded the axon collaterals.

In conclusion, we find that action potential invasion of the axonal arbour is reliable, even when the peak inward sodium current is reduced by application of a local anaesthetic. Thus action potential invasion of axon collaterals has a significant safety factor.

Bielefeldt K & Jackson MB (1993). *J Neurophysiol* **70**, 284–298.

Cox CL *et al.* (2000). *Proc Natl Acad Sci USA* **97**, 9724–9728.

Debanne D *et al.* (1997). *Nature* **389**, 286–289.

Stoppini L *et al.* (1991). *J Neurosci Meth* **37**, 173–182.

This work was supported by the BBSRC Bioimaging initiative.

All procedures accord with current UK legislation.

C27

Presynaptic cyclic nucleotide-gated ion channels modulate neurotransmitter release in mouse and rat olfactory bulb

Gabe J. Murphy and Jeffry S. Isaacson

Neuroscience Graduate Program, University of California, San Diego, La Jolla, CA 92093-0608, USA

In the dendritic cilia of olfactory receptor neurons (ORNs), cyclic nucleotides link stimulation of G protein-coupled odorant receptors to membrane depolarization by activating cyclic nucleotide-gated channels (CNGCs). CNGCs and odorant receptors may also be expressed in the nerve terminals of ORNs, where they have been proposed to contribute to the remarkably precise targeting of ORN axons to specific olfactory bulb glomeruli. Here we asked whether CNGCs in ORN nerve terminals modulate synaptic transmission.

Olfactory bulb slices (~300 μm) were prepared from 2- to 4-week-old Sprague-Dawley rats or c57bl6 mice in accordance with USA and institutional guidelines. Periglomerular (PG) neurons, which receive glutamatergic input from olfactory nerve (ON) fibres, were visualized via IR-DIC microscopy and patch clamped with electrodes containing a Cs-based internal solution. Data are presented as means ± S.E.M.

Bath application of forskolin (25–50 μM), an activator of adenylyl cyclase, or 8-Br-cGMP (500 μM), a membrane-permeable cGMP analogue, depressed the amplitude of ON-evoked EPSCs in PG neurons by 91.3 ± 1.9 % ($n = 5$) and 75.2 ± 1.3 % ($n = 5$), respectively. Forskolin and 8-Br-cGMP altered the frequency but not amplitude of mEPSCs, suggesting that cyclic nucleotides modulate transmission presynapticallly. To further address the specificity with which cyclic nucleotides altered synaptic transmission, we recorded glomerular field EPSPs evoked by ON and mitral cell stimulation. 8-Br-cGMP and forskolin inhibited ON- but not mitral cell-evoked fEPSPs, indicating that the effects of cyclic nucleotides were specific to ON-mediated transmission.

Curiously, the inhibition of ON-evoked fEPSPs by cyclic nucleotides occurred in parallel with an increase in presynaptic Ca^{2+}. Cyclic nucleotides largely abolished action potentials in ON fibres, an effect that was mimicked by applying an elevated (~7.5 mM) K^+ solution. These results suggest that cyclic nucleotides inhibit transmitter release by modulating the excitability of ON fibres.

To directly test whether the actions of cyclic nucleotides were due to CNGC activation, we examined the effects of cyclic nucleotides on synaptic transmission and ON excitability in mice lacking olfactory CNGCs. Cyclic nucleotides had no effect on transmission or ON excitability in CNGC mutant mice, indicating that the effects of 8-Br-cGMP and forskolin were attributable to CNGC activation. These results identify a novel role for CNGCs in neurotransmission.

G.J.M. is supported by an NRSA predocotoral fellowship from the NIH (NIDCD). J.S.I. is supported by a Burroughs-Welcome Fund Career Award, a McKnight Scholar award, and the NIH (NIDCD).

All procedures accord with current National and local guidelines.

C28

Sprouting of mossy fibres and involvement of presynaptic group II mGluRs in the dentate area of rat hippocampal slice cultures

Angharad Thomas, Francesco Ferraguti and Marco Capogna

MRC Anatomical Neuropharmacology Unit, Department of Pharmacology, University of Oxford, Oxford OX1 3TH, UK

Mossy fibre sprouting (MFS) is characterised by an abnormal projection of granule cell axon collaterals into the molecular layer of the dentate gyrus, where they form a recurrent excitatory network capable of promoting seizure-like activity.

This study aims to analyse the changes in granule cell excitability that occur in MFS and to investigate the involvement of presynaptic receptors at the sprouted synapses. We used organotypic slice cultures (obtained from 7-day-old rats killed according to Home Office regulations) since these cultures can display MFS (Zimmer & Gähwiler, 1984). First, we analysed the extent of MFS in cultures incubated for 7, 14 and 21 days *in vitro* (DIV), and then in cultures treated with the neurotoxic convulsant pilocarpine (0.5 mM) for 48 h at 5 DIV and tested at 21 DIV.

Timm staining revealed the presence of mossy terminals in the hilus and in a compact band along the stratum lucidum ($n = 45$). The density of staining in the hilus and molecular layer increased as a function of DIV. Pilocarpine treatment greatly enhanced the Timm stain in the molecular layer.

Whole-cell voltage-clamp recording of granule cells showed mEPSCs in the presence of 0.5 μM TTX and 30 μM bicuculline. The frequency of mEPSCs increased with DIV and was highest in pilocarpine-treated cultures ($n = 29$) (7 DIV, 0.28 ± 0.04; 14 DIV, 0.72 ± 0.08; 21 DIV*, 0.73 ± 0.05, pilocarpine treated*, 1.09 ± 0.03 (data shown as mean (Hz) ± S.E.M., * denotes significance with respect to 7 DIV, considered significant if $P < 0.05$, Student's t test)). Recorded granule cells were visualised by biocytin and a morphometric analysis revealed that the number of axon collaterals in the hilus was positively correlated with DIV, with the largest number in pilocarpine-treated cultures. 21 DIV control and treated cultures contained collaterals that extended into the granule and molecular layers.

Paired recordings of granule cells showed that pilocarpine-treated cultures had a larger proportion of monosynaptic and polysynaptic connections ($n = 59$). Monosynaptic unitary EPSCs had short latencies with a small jitter, were reliable and displayed paired-pulse depression. Application of the group II metabotropic glutamate receptor (mGluR) agonist LY354740 (0.5 μM) decreased the amplitude of EPSCs, elicited paired-pulse facilitation and increased the number of failures.

The excitability of granule cells in slice cultures is positively correlated with DIV, and pilocarpine treatment further enhances MFS and excitability. This study provides direct evidence for active connections between granule cells and demonstrates that presynaptic group II mGluRs are functional in the sprouted synapses.

Zimmer J & Gähwiler BH (1984). *J Comp Neurol* **228**, 432–446.

All procedures accord with current UK legislation.

C29

Role of endocannabinoids in metabotropic glutamate receptor-mediated depression of excitatory synaptic transmission in the adult rat hippocampus *in vitro*

Sam M. Greenwood and Stephen M. Fitzjohn

School of Biological Sciences, University of Manchester, 1.124 Stopford Building, Oxford Road, Manchester M13 9PT, UK

Release of endogenous cannabinoids decreases excitatory and inhibitory neurotransmission in several brain regions via activation of presynaptic type 1 cannabinoid receptors (CB1 receptors). Activation of group I metabotropic glutamate (mGlu) receptors is known to elicit release of these compounds and in the rodent hippocampus activation of group I mGlu receptors elicits a depression of excitatory synaptic transmission. Thus we were interested to see whether mGlu-receptor-mediated synaptic depression involves the release endocannabinoids which then act as retrograde messengers to stimulate CB1 receptors. Standard *in vitro* extracellular recordings of fEPSPs were made from area CA1 of hippocampal slices prepared from female Wistar rats (10–13 weeks of age). Rats were killed in accordance with the UK Animals (Scientific Procedures) Act, 1986. Application of the group I mGluR agonist DHPG (100 μM) elicited an acute decrease in fEPSPs to 40 ± 8 % of control (mean ± S.E.M.; $n = 8$) that reversed only partially upon washout of DHPG (responses 60 min after washout of DHPG were 79 ± 7 % of control; $P < 0.05$, Student's paired t test). Delivery of a low-frequency train of paired-pulse stimuli (PP-LFS; 900 paired stimuli at 1 Hz, inter-pulse interval 50 ms) induced a long-term depression (LTD) of synaptic transmission (responses 60 min after delivery of PP-LFS were 80 ± 4 % of control; $n = 4$; $P < 0.05$), which is known to be dependent upon activation of group I mGlu receptors. However, neither DHPG-induced depression nor LTD induced by PP-LFS was prevented by application of the CB1 receptor antagonist AM251 (500 nM). In the presence of AM251, DHPG depressed fEPSPs to 68 ± 13 % of control ($n = 4$; $P > 0.05$ compared with depression obtained in the absence of AM251, Student's unpaired t test), and 60 min after washout of DHPG responses were 84 ± 5 % of control. PP-LFS in the presence of AM251 resulted in a reduction of fEPSPs to 81 ± 4 % of control ($n = 4$; $P > 0.05$). Thus it appears that release of endocannabinoids and subsequent activation of CB1 receptors is not involved in the induction of these forms of mGlu receptor-dependent depression in the adult rat hippocampus. If, as has been postulated, activation of postsynaptic group I mGlu receptors produces a presynaptic depression in glutamate release, then some other form of retrograde messenger must be involved.

All procedures accord with current UK legislation.

C30

Vesicular release of GABA contributes to both phasic and tonic inhibition of granule cells in the mature cerebellum of mice

Stephen G. Brickley, Stuart G. Cull-Candy and Mark Farrant

Department of Pharmacology, University College London, London WC1E 6BT, UK

We have previously described two distinct modes of $GABA_A$ receptor activation in cerebellar granule cells (GCs) – the phasic activation of synaptic $GABA_A$ receptors following vesicular GABA release and a tonic conductance arising from the persistent activation of extrasynaptic $GABA_A$ receptors by low concentrations of ambient GABA (Brickley *et al.* 1996). Recent studies have suggested that in the mature rat cerebellum spontaneous $GABA_A$ receptor-mediated synaptic currents (sIPSCs) are rare and the GABA giving rise to the tonic conductance is not produced by conventional vesicular release from Golgi cell interneurons (Wall & Usowicz, 1997; Hamann *et al.* 2002). These observations have called into question the function of both phasic and tonic inhibition in the dynamic control of granule cell excitability (De Schutter, 2002).

We made whole-cell recordings from GCs in slices prepared from 7- to 200-day-old mice (P7–P200) in accordance with the UK Animals (Scientific Procedures) Act, 1986, as described previously. Across all ages, over 80 % of GCs exhibited sIPSCs (186 out of 221 GCs in 64 animals). Even at P200 sIPSCs were readily detected, occurring at a frequency of 0.8 ± 0.3 Hz (mean ± S.E.M.) in six out of seven GCs, similar to the situation previously reported in P35 animals (Brickley *et al.* 2001). In mature animals, addition of TTX (1 μM) or removal of external Ca^{2+} resulted in a significant reduction in the frequency of IPSCs (average age P66 ± 14, $n = 22$). The miniature IPSCs that remained in the presence of TTX occurred at a frequency of 0.09 ± 0.02 Hz. This reduction in vesicular GABA release following TTX application or Ca^{2+} removal also resulted in a 56 ± 7 % ($n = 15$) reduction in the tonic $GABA_A$ receptor-mediated conductance in mature GCs. This result contrasts with previous reports that the tonic conductance was TTX insensitive (Wall & Usowicz, 1997; Hamann *et al.* 2002).

In conclusion, action potential-dependent release of GABA from cerebellar Golgi cells occurred at all ages. Reduction in vesicular GABA release affected not only the frequency of phasic IPSCs but also the magnitude of the tonic $GABA_A$ receptor-mediated conductance. Therefore, the overall level of Golgi cell activity will modulate both phasic and tonic inhibition in mature GCs, an observation which is consistent with current theories of cerebellar function (De Schutter, 2002).

Brickley SG *et al.* (1996). *J Physiol* **497**, 753–759.

Brickley SG *et al.* (2001). *Nature* **409**, 88–92.

De Schutter E (2002). *Curr Biol* **12**, R363–365.

Hamann M *et al.* (2002). *Neuron* **33**, 625–633.

Wall MJ & Usowicz MM (1997). *Eur J Neurosci* **9**, 533–548.

This work was supported by The Wellcome Trust.

All procedures accord with current UK legislation.

C31

The α-latrotoxin mutant LTX^{N4C}, which does not form ionic pores, enhances spontaneous and evoked transmitter release in rat CA3 pyramidal neurons

Marco Capogna*, Kirill E. Volynski†, Nigel J. Emptage‡ and Yuri A. Ushkaryov†

**MRC Anatomical Neuropharmacology Unit, Department of Pharmacology, University of Oxford, Oxford OX1 3TH, UK, †Department of Biological Sciences, Imperial College, London SW7 2AY, UK and ‡Department of Pharmacology, University of Oxford, Oxford OX1 3TH, UK*

α-Latrotoxin (LTX) stimulates vesicular exocytosis by at least two mechanisms that include (i) receptor binding/stimulation and (ii) membrane pore formation. Here, we use the toxin mutant, LTX^{N4C}, produced by the insertion of four amino acids

into the native sequence, to selectively study the receptor-mediated actions of LTX.

LTX^{N4C} bound to both LTX receptors (latrophilin 1 and neurexin Iα) and greatly increased the frequency of mEPSCs recorded in whole-cell voltage-clamp mode from CA3 pyramidal neurons in rat hippocampal slice cultures (23.5 ± 5-fold, $n = 18$, $P < 0.001$ (data shown as means ± S.E.M., paired t test, considered significant if $P < 0.05$)). LTX^{N4C} acted only via the receptor-mediated mechanism because it failed to form tetramers and ionic pores and its effect was reversible and was not inhibited by La^{3+} which, in agreement with previous observations (Ashton *et al.* 2001), perturbed LTX pores.

The action of LTX^{N4C} on mEPSCs was attenuated by the removal of extracellular Ca^{2+} and by the inhibition of phospholipase C with U73122 (4.2 ± 1.3-fold, $n = 5$, $P < 0.02$ and 5 ± 1.5-fold, $n = 4$, $P < 0.05$, respectively). Furthermore, both thapsigargin, which depletes Ca^{2+} stores, and 2-aminoethoxydiphenyl borate, which blocks IP_3-induced release of Ca^{2+} from such stores, essentially abolished the LTX^{N4C}-evoked increase in mEPSC frequency (2 ± 0.5-fold, $n = 5$, $P > 0.7$ and 2.1 ± 0.5-fold, $n = 9$, $P > 0.08$, respectively).

Measurements using a fluorescent Ca^{2+} indicator directly demonstrated that LTX^{N4C} increased the basal fluorescence at axonal varicosities ($n = 6$, $P < 0.03$); this rise of cytosolic Ca^{2+} was prevented by thapsigargin ($n = 3$, $P > 0.5$), suggesting, together with electrophysiological data, that the receptor-mediated action of LTX^{N4C} involved the mobilization of Ca^{2+} from intracellular stores.

Finally, in contrast to the wild-type LTX, which inhibited evoked synaptic transmission probably due to pore formation, LTX^{N4C} actually enhanced synaptic currents elicited by electrical stimulation of afferent fibres (1.4 ± 0.1-fold, $n = 5$, $P < 0.04$).

We suggest that the mutant LTX^{N4C}, lacking the ionophore-like activity of the wild-type toxin, activates a presynaptic receptor, probably the G protein-coupled latrophilin 1, and stimulates phospholipase C, leading to subsequent Ca^{2+} release from intracellular stores and the enhancement of synaptic vesicle exocytosis.

Ashton AC *et al.* (2001). *J Biol Chem* **276**, 44695–44703.

This work was supported by the MRC and Wellcome Trust.

All procedures accord with current UK legislation.

C32

Synaptotagmin self-oligomerization is not absolutely required for fast transmission at mouse hippocampal synapses

Catherine R. Borden, Jane M. Sullivan and Charles F. Stevens

Salk Institute, MNL-S, 10010 North Torrey Pines Road, La Jolla, CA 92037, USA

Synaptotagmin I, an integral synaptic vesicle protein, is the putative calcium sensor for fast, synchronous transmission. *In vitro*, synaptotagmin shows calcium-dependent self-oligomerization and binding to both phospholipids and SNARE (soluble NEM-sensitive factor attachment protein receptor) proteins. Each of these interactions has been postulated to be crucial to synaptotagmin's role as the calcium sensor, but direct evidence is sparse. We have tested the importance of self-oligomerization to the calcium-sensing mechanism by recording from neurons that express only oligomerization-deficient synaptotagmin.

Hippocampal cell cultures were prepared from synaptotagmin I knock-out mice at embryonic day 18, in accordance with USA and institutional guidelines. After 9–16 days, neurons were infected with Semliki Forest Virus constructs (Invitrogen) containing genes for a synaptotagmin mutant and enhanced green fluorescent protein as a reporter. Whole-cell voltage-clamp recordings were made 8–24 h later from autaptic neurons grown on microislands.

Two different synaptotagmin mutants were used to test the importance of self-oligomerization. One contains an asparagine (N) residue in position 311 instead of a tyrosine (Y). Biochemical studies with the Y311N mutant show a complete lack of calcium-dependent self-oligomerization, while binding to SNARE proteins and phospholipids is normal (Littleton *et al.* 2001).

In the second mutant, lysines in positions 326 and 327 are mutated to alanines. This K326, 327A mutant also lacks calcium-dependent self-oligomerization *in vitro*, while binding to SNARE proteins is normal (Earles *et al.* 2001).

If self-oligomerization is essential for synaptotagmin to work, then these mutants should not be able to support fast synaptic transmission. When neurons were transfected with either mutant, however, they showed clear EPSCs, as did wild-type transfected controls. Thus our results do not support the proposal that self-oligomerization, as determined in biochemical studies, is essential for synaptotagmin's role as the calcium sensor for neurotransmission.

Earles CA *et al.* (2001). *J Cell Bio* **154**, 1117–1123.

Littleton JT *et al.* (2001). *J Neurosci* **21**, 1421–1433.

This work was supported by the Howard Hughes Medical Institute (C.F.S.) and Merck and Chapman Fellowships (C.R.B.).

All procedures accord with current National and local guidelines.

C33

Release probability-dependent changes of the AMPA receptor EPSC waveform at the rat cerebellar mossy fibre to granule cell synapse

T.A. Nielsen, D.A. DiGregorio and R.A. Silver

Department of Physiology, University College London, London WC1E 6BT, UK

At many glutamatergic synapses, the decay of the EPSC accelerates as the release probability is lowered (Trussel *et al.* 1993; Mennerick & Zorumski, 1995; Silver *et al.* 1996). This non-linearity is thought to arise from spillover of glutamate between neighbouring active zones, but the mechanism by which this is achieved is unclear. We have investigated this issue by combining electrophysiological recordings from the cerebellar mossy fibre to granule cell synapse, where spillover currents can be observed in isolation (DiGregorio *et al.* 2002), with a model of glutamate diffusion.

Thin parasagittal slices were cut from the vermal cerebellum from P25 rats killed by decapitation. Whole-cell patch-clamp recordings were made from granule cells, and mossy fibres were stimulated extracellularly (Silver *et al.* 1996). We recorded pharmacologically isolated non-NMDA currents at 36–37 °C. Diffusion in the synaptic cleft was simulated using an analytical solution to Fick's second law for the region bound by two parallel planes (Otis *et al.* 1996) with stochastic release from 25 sites.

The acceleration of the EPSC in lowered $[Ca^{2+}]_o$ was quantified by the weighted decay, determined from the integral of the peak-

normalised EPSC. Relative to $[Ca^{2+}]_o = 2$ mM, the weighted decay was reduced to 96 ± 5.8, 89 ± 7.4 and 82 ± 9.0 % in $[Ca^{2+}]_o = 1.5$, 1.25 and 1 mM, respectively (means ± S.E.M., $n = 13$). Simulations of glutamate diffusion following the stochastic release of quanta of neurotransmitter indicated that the release probability determines the amplitude but not the mean waveform of the glutamate transient. Simulations indicated that the glutamate concentration due to spillover attained on a particular trial is likely to be proportional to the release probability (Pearson correlation coefficient = 0.94), and thus to the peak EPSC amplitude. The isolated spillover current, when plotted against the peak EPSC amplitude for each $[Ca^{2+}]_o$ could be fitted with a Hill equation, giving a mean Hill coefficient of 1.46 ± 0.14 ($n = 9$) for synaptic receptors. This value is close to previous estimates from patches, consistent with the acceleration being due to non-linear activation of postsynaptic receptors.

DiGregorio DA *et al.* (2002). *Neuron* **35**, 521–533.

Mennerick S & Zorumski CF (1995). *J Neurosci* **15**, 3178–3192.

Otis TS *et al.* (1996). *J Neurosci* **16**, 1634–1644.

Silver RA *et al.* (1996). *J Physiol* **494**, 231–250.

Trussell LO *et al.* (1993). *Neuron* **10**, 1185–1196.

This work was supported by The Wellcome Trust and the European Commision. R.A.S. is the recipient of a Wellcome Trust Senior Research Fellowship.

All procedures accord with current UK legislation.

C34

Ascending granule cell axon synapses onto rat Purkinje cells have different transmission properties from those made by parallel fibres

Robert E. Sims and Nicholas A. Hartell*

*School of Life and Health Sciences, Aston University, Aston Triangle, Birmingham B4 7ET and *Department of Pharmacology, The School of Pharmacy, University of London, London WC1N 1AX, UK*

Cerebellar Purkinje cells (PCs) are innervated by granule cells (GCs) whose axons ascend into the molecular layer where they bifurcate to form parallel fibres (PFs). These extend laterally for several millimetres in both directions. Transmission of information along PFs to PCs may be more limited than previously thought (Cohen & Yarom, 1998). Moreover, synapses made by ascending axon segments onto PCs have a greater presynaptic vesicle density than PF synapses, suggesting a greater synaptic weight (Gundappa-Sulur *et al.* 1999). We have therefore compared the transmission properties of synapses formed onto PCs by ascending segments of granule cell axons and PFs.

Coronal cerebellar slices (250 μm thick) were prepared from the brains of 14- to 21-day-old male Wistar rats decapitated under isofluorane anaesthesia (inhalation). Whole-cell recordings were made from Purkinje cell somata voltage clamped at −70 mV at room temperature in the presence of 20 μM picrotoxin. One stimulating pipette was placed in the GC layer, directly below the recorded PC to activate ascending axon synapses. A second pipette was placed in the ML, 100 μm laterally, to activate PF synapses. All results are presented as means ± S.E.M.

Pairs of stimuli (50 ms interval) were applied to each pathway alternately at 0.2 Hz. The level of paired pulse facilitation of ML response (1.94 ± 0.06) was significantly higher than GC responses (1.59 ± 0.08; Mann-Whitney U test, $P < 0.05$, $n = 6$). Variance-mean analysis (Clements & Silver, 2000) performed under four different experimental conditions of release probability revealed that synapses activated by GC layer stimulation displayed a higher quantal content than those activated by ML stimulation (GL, 10.4 pA; ML, 7.7 pA) and a greater release probability (GL, 0.39; ML, 0.26; at 2.5 mM Ca^{2+}).

Analysis of responses to trains of up to seven stimuli (50 ms interval) in 1 mM Ca^{2+} and the presence and absence of the AMPA receptor antagonist 2,3-dioxo-6-nitro-1,2,3,4-tetrahydrobenzo[f]qunioxaline-7-sulfonamide (NBQX) was conducted. NBQX (75 nM) reduced GL and ML responses to 56 ± 6 and 50 ± 2 %, respectively, of control values. The derived quantal amplitudes fell to 54 ± 12 and 56 ± 8 % of baseline levels, indicating a proportionally similar effect on AMPA receptors at both pathways. These data reveal fundamental differences in transmission properties between synapses made onto PCs by different segments of the same GC axons.

Clements JD & Silver RA (2000). *TiNS* **23**, 105–113.

Cohen D & Yarom Y (1998). *PNAS* **95**, 15032–15036.

Gundappa-Sulur G *et al.* (1999). *J Comp Neurol* **408**, 580–596.

All procedures accord with current UK legislation.

C35

Does nitric oxide regulate the NMDA receptor?

R.A. Hopper and J. Garthwaite

Wolfson Institute for Biomedical Research, University College London, Gower Street, London WC1E 6BT, UK

Nitric oxide (NO) functions as a messenger throughout the central nervous system, where many of its actions are exerted through guanylyl cyclase activation, leading to cGMP formation. A putative alternative transduction pathway is the modification of protein function by nitrosation of thiol groups (Ahern *et al.* 2002). A prototypic protein considered to be regulated in this way is the NMDA receptor but, despite extensive research, there is little direct evidence that NO performs this function. To address this issue, we have investigated the effect of NO on native or cloned NMDA receptors (NMDARs) in hippocampal slices and HEK-293 cells, respectively.

Field EPSPs were recorded from the CA1 stratum radiatum of hippocampal slices obtained from 6- to 8-week-old rats killed humanely according to Home Office regulations (Bon & Garthwaite, 2001). EPSPs mediated through NMDARs were isolated pharmacologically. The responses were not significantly changed by bath application of the NO synthase substrate, L-arginine (100 μM), nor by inhibition of NO synthase using L-nitroarginine (100 μM). Diethylamine NO adduct (DEA/NO) was used to supply NO exogenously. Whilst DEA/NO at a concentration of 10 μM caused maximal cGMP accumulation in hippocampal slices, concentrations up to 30-fold higher produced no detectable change in the NMDAR-mediated synaptic responses. However, in accordance with a previous study (Murphy *et al.* 1994), photolysis of a caged NO derivative using a flash of UV light depressed NMDAR-mediated EPSPs by 94 ± 3 % (mean ± S.E.M.; $n = 4$).

As a further test, whole-cell membrane currents in response to 100 ms pulses of 100 μM glutamate were recorded at −60 mV from HEK-293 cells transfected with NMDAR subunits NR1 and NR2A (Köhr & Seeburg, 1996). Similar to findings in the slices, photolysis of the caged compound by UV light depressed the NMDAR currents by 55 ± 3% ($n = 5$), whereas 100 μM DEA/NO had no significant effect on the NMDAR current alone, but depressed the NMDAR currents by 35 ± 7% ($n = 4$) when in

combination with UV light. Perfusion of 100 nM DEA/NO had no effect on NMDAR function.

The results suggest that NO released endogenously, or exogenous NO in concentrations well in excess of those needed to activate guanylyl cyclase, does not modify NMDAR function. It is possible that other factors, such as UV light, may have contributed to the inhibition of NMDAR responses observed previously (Murphy *et al.* 1994).

Ahern GP *et al.* (2002). *Trends Neurosci* **25**, 510–517.

Bon CLM & Garthwaite J (2001). *Eur J Neurosci* **14**, 585–594.

Köhr G & Seeburg PH (1996). *J Physiol* **492**, 445–452.

Murphy KPSJ *et al.* (1994). *Neuropharmacology* **33**, 1375–1385.

This work was supported by a BBSRC CASE studentship with Merck Sharp and Dohme (Harlow, UK) and The Wellcome Trust. We thank Dr B. Lancaster for expert advice.

All procedures accord with current UK legislation.

C36

Kinetics of nitric oxide inactivation in rat brain

C. Hall, C. Griffiths and J. Garthwaite

Wolfson Institute for Biomedical Research, University College London, London WC1E 6BT, UK

Nitric oxide (NO) is an intercellular messenger in the brain, where it stimulates guanylyl cyclase, producing cGMP. The NO-cGMP pathway is involved in many physiological functions but at high levels, and through other mechanisms, NO can also be toxic. The regulation of the NO concentration is, therefore, critical. Whilst NO formation through NO synthases is now well established, it has only recently become apparent that brain (and other tissue) also possesses a powerful NO consuming activity (Griffiths & Garthwaite, 2001). This study aimed to determine the kinetic properties of the NO inactivating pathway in brain tissue.

The experiments used either dispersed cells or intact slices from the cerebellum of 8-day-old rats that had been killed humanely in accordance with Home Office regulations. In the dispersed cells, application of 0–250 μM diethylaminetriamine/NO adduct led to differing steady-state NO concentrations, from which the inactivation rates were determined. These followed Michaelis-Menten kinetics, yielding a K_m of 62 nM and a V_{max} of 0.43 nmol (mg protein s)$^{-1}$.

Experiments were carried out on cerebellar slices to evaluate the rate of NO inactivation in more physiological brain tissue. The steady-state levels of cGMP provided an index of the penetration of NO into the slices when they were bathed in solutions containing various fixed NO concentrations (generated using appropriate donors). As predicted should the inward diffusion of NO be limited by NO consumption, half-maximal cGMP accumulation required an external NO concentration of 1.0 μM, which is 500-fold higher than that required in dispersed cerebellar cells. Also as predicted, cGMP immunocytochemistry indicated that, at lower external NO concentrations, marked gradients of NO existed across the slice thickness at steady state. This approach further suggested that the rate of inactivation of NO was grossly similar in different regions of the cerebellum. Application of a simplified diffusion model to the data suggested that the V_{max} value for intact cerebellar tissue is at least 1 μM s^{-1}, which is about 2-fold higher than the value predicted from the isolated cells after correcting for the different protein concentrations.

The kinetic properties of the NO inactivation pathway suggest that, when NO release rates are low, the mechanism serves to translate those release rates rapidly (under 40 ms time scale) into proportionate NO concentrations constrained to target guanylyl cyclase (0.5–20 nM). At higher NO release rates, the inactivation pathway would be instrumental in preventing toxic NO concentrations (> 100 nM) being attained under normal conditions.

Griffiths CG & Garthwaite J (2001). *J Physiol* **563**, 855–862.

This work was supported by The Wellcome Trust and the Sir Jules Thorn Charitable Trust.

All procedures accord with current UK legislation.

C37

Characterization of NMDA receptor subtypes in rat substantia nigra dopamine cells

Alasdair J. Gibb* and Susan Jones†

**Department of Pharmacology, University College London and †Department of Anatomy, University of Cambridge, Cambridge, UK*

NMDA glutamate receptors (NMDARs) on substantia nigra *pars compacta* (SNc) dopamine cells possibly contribute to excitotoxic neurodegeneration of dopamine cells in Parkinson's disease and are therefore potential therapeutic targets. We have used patch-clamp recording methods to identify NMDAR subtypes present in excised, outside-out patches from dopamine cells in 300 μm coronal slices of SNc from humanely killed rats (postnatal days 14–16).

Single-channel recordings of NMDAR channels activated by 100 nM NMDA and 10 μM glycine were analysed to determine which subunits form functional NMDARs in SNc dopamine cells. Distributions of channel amplitudes identified four conductance levels (18, 27, 37 and 49 pS) in 11 of 13 patches. Direct transitions between 37 and 18 pS conductance levels exhibited asymmetry in the frequency of transitions between the two conductance states, indicating that NR2D subunits, rather than NR2C subunits contribute to these receptors (Wyllie *et al.* 1996). The NR2B antagonist ifenprodil (1 μM) reduced P_{open} by 41.1 ± 8.8 % (mean ± S.E.M., $n = 7$ patches) but, unexpectedly, this effect was not selective for only high conductance channels. Ifenprodil reduced equally the activity of all conductance levels, suggesting that the NR2B subunit contributes to both high and low conductance receptors. Channel activity was not sensitive to 50 nM Zn^{2+} or 1 μM TPEN (*N, N, N′, N′*-tetrakis(2-pyridyl-methyl)ethylenediamine), a high-affinity zinc chelating agent, suggesting that NR2A subunits do not contribute to these receptors. These data suggest that functional NMDARs on SNc dopamine cells in 2-week-old rats are heterotrimers composed of NR1, NR2B and NR2D subunits.

Wyllie DJ *et al.* (1996). *Proc R Soc Lond* B **263**, 1079–1086.

This work was supported by the MRC and Wellcome Trust. S.J. is supported by the Parkinson's Disease Foundation and the National Parkinson's Foundation.

All procedures accord with current UK legislation.

C38

One quarter of NMDA receptors on CA1 pyramidal cells could detect glutamate release at more than one synapse

Annalisa Scimemi and Dmitri A. Rusakov

Institute of Neurology, University College London, Queen Square, London WC1N 3BG, UK

Evidence for glutamate spillover in the hippocampus at physiological temperature remains controversial. We recorded from CA1 pyramidal cells (whole-cell mode) in acute hippocampal slices (obtained from young adult rats killed by decapitation) at 35 °C. We examined synaptic events mediated by NMDA receptors (NMDARs) by holding cells at +40 mV in the presence of CNQX. We divided stratum radiatum into two separate pathways that converged on the same cell but could be stimulated independently. After obtaining stable responses to single stimuli at each pathway, we applied the use-dependent NMDAR blocker MK801 and continued stimulation of only one (test) pathway until the EPSCs decreased to ~15 % of baseline. When we resumed stimulation of the other (silent) pathway, its responses were reduced to 48 ± 7 % (mean ± S.E.M.) of baseline ($n = 7$). This reduction could not be explained by the spontaneous activation of NMDARs in the presence of MK801: the latter reduced EPSCs only to 71 ± 6 % of baseline in control experiments ($n = 15$). Nor could it be explained by the activity-dependent changes in the occupancy of the NMDAR glycine-binding sites: 100 μM D-serine had no effect on the MK801-dependent reduction of EPSCs ($n = 6$). However, the MK801-dependent block of NMDARs at the silent pathway was exacerbated ~4-fold when glutamate uptake was blocked ($n = 7$), and ~2-fold when five stimuli at 50 Hz were applied to the test pathway ($n = 8$). Assuming that MK801 blocks the proportion p of NMDAR channels upon each stimulus, the normalised amplitude of NMDAR EPSCs at the nth stimulus is $(1 - p)^n$. Our data then indicate that, on average, ~25 % of NMDARs at pyramidal cells can be activated by glutamate released at more than one synapse supplied by stratum radiatum. We also simulated extracellular glutamate diffusion in a 3D synaptic scatter compatible with neuropil in area CA1: the results provided quantitative insights into the relationship between synaptic activation and the extent of spatial glutamate 'pools' in the extracellular space.

All procedures accord with current UK legislation.

C39

NMDAR channels in cerebellar Golgi cells of wild-type and NR2D subunit ablated mice

Charu Misra*, Stephen G. Brickley*, M.H. Selina Mok*, Masayoshi Mishina† and Stuart G. Cull-Candy*

**Department of Pharmacology, University College London, Gower Street, London WC1E 6BT, UK and †Department of Molecular Neurobiology and Pharmacology, University of Tokyo, Tokyo 113–0033, Japan*

NMDA receptor (NMDAR) assemblies consist of NR1 subunits combined with at least one type of NR2 subunit (NR2A-D). NMDAR functional diversity arises largely from differences in NR2 subunit composition. For example, in cerebellar Golgi cells it is thought that NR1/NR2B and NR1/NR2D subunit-containing receptors give rise to high- (40–50 pS) and low-conductance (20–40 pS) single-channel openings, respectively (Misra *et al.* 2000). Further functional diversity could arise if more than one type of NR2 subunit coexists within a *native* receptor. We have used NR2D subunit ablated animals, to determine whether NR2B and NR2D subunits co-assemble in Golgi cells to form a distinct receptor subtype.

Parasaggital cerebellar slices were prepared from 8- to 10-day-old C57BL/6J mice (wild-type, WT), and NR2D subunit ablated (NR2D −/−) mice killed by decapitation (Ikeda *et al.* 1995). In outside-out patches from WT animals, application of 10 μM NMDA elicited a mixture of high- and low-conductance channels, while patches from NR2D −/− mice produced only high-conductance events. We next compared the biophysical and pharmacological properties of high-conductance (50 pS) openings in isolation. The mean single-channel conductance of these events was no different in the two strains, but the probability of opening ($P_{open(HIGH)}$) was greater in NR2D −/− (0.04 ± 0.004, mean ± S.E.M.) than in WT (0.02 ± 0.004; $P < 0.05$, Student's t test). As the NR2D subunit confers a low probability of opening, when combined with NR1 (Wyllie *et al.* 1996) our results suggest the presence of the NR2D subunit in some high-conductance NR2B-containing assemblies in WT mice. Furthermore, the NR2B subunit-selective antagonist ifenprodil reduced $P_{open(HIGH)}$ by only 31.2 ± 9.4 % ($n = 7$) in WT, compared with 52.4 ± 9.3 % ($n = 9$; $P < 0.05$) in NR2D −/− mice. This is consistent with the presence of an ifenprodil-insensitive NR2D subunit within NR2B subunit-containing NMDAR complexes in the WT.

In conclusion, our results indicate that deletion of the NR2D subunit results in a loss of low-conductance NMDAR channels, while the conductance of the remaining openings was unaltered. Furthermore, changes in the biophysical and pharmacological properties of the remaining 50 pS openings, suggests that a novel triheteromeric receptor subtype, containing both NR2B and NR2D subunits, was present in the WT.

Ikeda K *et al.* (1995). *Brain Res Mol Brain Res* **33**, 61–71.

Misra C *et al.* (2000). *J Physiol* **524**, 147–162.

Wyllie DJA *et al.* (1996). *Proc R Soc Lond* B **263**, 1079–1086.

This work was supported by The Wellcome Trust.

All procedures accord with current UK legislation.

C42

Modulation of AMPA receptors by external inorganic cations

L.G. Magazanik, N.A. Dorofeeva and D.B. Tikhonov

Sechenov Institute of Evolutionary Physiology and Biochemistry RAS, St Petersburg, Russia

The effect of extracellular ionic contents on the Ca^{2+}-impermeable AMPA receptors of hippocampal pyramidal neurons has been studied using the patch-clamp technique. Neurons were isolated from rats decapitated under urethane anaesthesia. Divalent cations produced fast concentration-dependent inhibition of currents evoked by 100 μM kainate. The IC_{50} (mean ± S.D.) values were: Ni^{2+}, 0.42 ± 0.02; Zn^{2+}, 1.1 ± 0.2; Co^{2+}, 6.1 ± 0.1; Ca^{2+}, 8.1 ± 0.3; $Mn^{2+} > 20$ and $Mg^{2+} > 40$ mM. The blocking effects were voltage-independent and can be prevented by 100 μM of cyclothiazide, which allosterically potentiates AMPA receptors. This suggests that divalent cations modulate activation or desensitization properties of the AMPA receptor rather than affect the ion channel. Acidification of the external media produces similar effects (Ihle & Patneau, 2000);

the IC_{50} value for proton inhibition of AMPA receptors in our experiments was 0.01 ± 0.006 ($pH_{50} = 6.2$). The action of Ni^{2+} and Ca^{2+} at pH = 6.0 and pH = 7.3 have been compared (Fig. 1). Significant decrease of the slope of concentration–response curve at lower pH suggests that inhibition by protons and divalent cations is interrelated. We propose cooperative action of divalent ions and protons at the homologous sites.

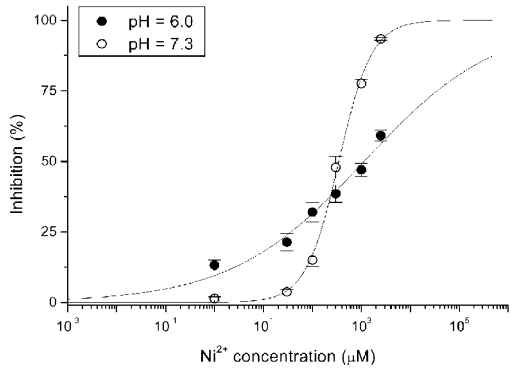

Figure 1. pH dependence of Ni^{2+} inhibition of AMPA receptors.

Divalent cations induce a parallel shift of the kainate concentration–response curve; at high kainate concentrations (3 mM) IC_{50} values of divalent cations become much higher. Therefore, cyclothiazide, which is known to increase affinity of agonists to AMPA receptors (Partin *et al.* 1996), is able to prevent inhibition by inorganic cations. Presently it is not clear how competitive-like binding of kainic acid and inorganic cations occurs. Possibly, cations have specific binding sites in the cleft between agonist-binding domains of the AMPA receptor, where binding sites for agonists and classical competitive antagonists are located (Armstrong & Gouaux, 2000).

These results show that activation of the AMPA receptor is not determined by intrinsic features of the receptor only, but depend on the ionic environment. It is unlikely that variations of extracellular ionic content required for significant change of AMPA receptor properties occur under physiological conditions. However, in some experiments the ionic content is substantially changed, and possible effect of such substitutions on AMPA receptors should be taken into account. It would also be interesting to compare determinants and mechanism of action of cations on AMPA and NMDA receptors, for which modulations by Zn^{2+} and protons is thought to be of physiological importance.

Armstrong N & Gouaux E (2000). *Neuron* **28**, 165–181.
Ihle EC & Patneau DK (2000). *Mol Pharmacol* **58**, 1204–1212.
Partin KM *et al.* (1996). *J Neurosci* **16**, 6634–6647.

This work was supported by RFBR 00-15-97987, 01-04-49353.

All procedures accord with current National and local guidelines.

C43

Stoichiometry of rat recombinant heteromeric glycine receptors: a mutation approach

Valeria Burzomato, P.J. Groot-Kormelink, L.G. Sivilotti and M. Beato*

*Pharmacology, The School of Pharmacy, London WC1N 1AX and *University College London, London WC1E 6BT, UK*

Adult glycine receptors are pentamers of $\alpha 1$ and β subunits but their stoichiometry is still controversial. Knowing the stoichiometry of heteromeric glycine receptors is an essential starting point for any functional and kinetic study, since the number of α subunits provides an upper limit to the number of binding sites present. In order to assess the stoichiometry we mutated the 9′ residue of the pore lining domain of $\alpha 1$ and β subunits from a conserved hydrophobic leucine into a hydrophilic threonine. Such mutation results in a leftward shift in the agonist dose–response curves for all channels in the nicotinic superfamily tested (Boorman *et al.* 2000).

HEK 293 cells were transfected with $\alpha 1$ and β cDNA in a 1:40 ratio in order to minimize contamination by homomeric $\alpha 1$ receptors. Glycine responses were recorded in whole-cell patch clamp from cells transfected with wild-type $\alpha 1\beta$, $\alpha 1\beta^{LT}$ and $\alpha 1^{LT}\beta$ subunits. EC_{50} and Hill slope values were obtained by fitting dose–response curves with the Hill equation. EC_{50} values of mutant receptors were lower than the wild-type value of 92 ± 4 μM (mean ± S.E.M., $n = 7$), particularly for $\alpha 1^{LT}\beta$ (1.3 ± 0.1 μM, $n = 11$; cf. 18 ± 4 μM, $n = 12$ for $\alpha 1\beta^{LT}$).

This change is accompanied by a decrease in the Hill slope, from 2.0 ± 0.1 for the wild-type to 1.5 ± 0.1 and 1.2 ± 0.1 for $\alpha 1\beta^{LT}$ and $\alpha 1^{LT}\beta$, respectively. In order to compare EC_{50} changes, dose–response curves were normalized to their maxima and averaged. When the three curves were fitted with the constraint of parallelism, the common Hill slope was 1.5, while the EC_{50} decreased 10.1- and 74.5-fold for $\alpha 1\beta^{LT}$ and $\alpha 1^{LT}\beta$, respectively.

If the effect of the mutation is independent of which subunit carries it, our data show that there are more copies of $\alpha 1$ than β. This is in contrast with nicotinic and GABA receptors, which have only two copies of the main agonist binding subunit. Either a 4:1 or a 3:2 stoichiometry is possible. However, the former is not in agreement with the observation that in other channels in this superfamily each copy of this mutation produces the same amount of shift in the EC_{50} and that such shifts are additive, namely:

$$\sqrt[n]{(EC_{50,wt}/EC_{50,n})} = \sqrt[m]{(EC_{50wt}/EC_{50,m})}.$$

Thus if n is the number of $\alpha 1$ and m the number of β subunits, for a 4:1 stoichiometry, the values observed would give $(74.5)^{1/4} = 2.9$ and $(10.1)^{1} = 10.1$. On the contrary, for a stoichiometry of 3:2 our data yield $(74.5)^{1/3} = 4.2$ and $(10.1)^{1/2} = 3.2$. This finding is also in agreement with the conclusions of Kuhse *et al.* (1993) based on the expression of chimaeric receptor subunits.

Boorman JP *et al.* (2000). *J Physiol* **529**, 565–577.
Kuhse J *et al.* (1993). *Neuron* **11**, 1049–1056.

This work was supported by the MRC and The Wellcome Trust (project grant 064652).

C44

Single-channel analysis of ϵL78P, a mutation responsible for slow channel congenital myasthenia

Chris Shelley*, Martyn Brydson†, David Beeson† and David Colquhoun*

**Department of Pharmacology, University College London, London WC1E 6BT and †Neurosciences Group, Institute of Molecular Medicine, John Radcliffe Hospital, Oxford OX3 9DU, UK*

Slow channel congenital myasthenic syndrome is a rare muscle disease resulting in muscle weakness and the degradation of muscle endplates. The condition is caused by single point mutations in muscle nicotinic ACh receptor subunits. One such mutation, ϵL78P, is responsible for a mild form of the disease (Croxen *et al.* 2002) and has been investigated at the single-channel level to elucidate the effects of the mutation on channel kinetics. Single-channel recordings were made in the cell-attached configuration of HEK293 cells transfected transiently with cDNA encoding enhanced green fluorescent protein, human α, β, δ, and either wild-type ϵ or ϵL78P nicotinic receptor subunits. The receptor with ϵL78P produced longer bursts of openings than wild-type channels. For both types of channel the burst length distribution could be fitted with four exponential components (100 nM ACh, −100 mV, resolution 25–35 μs). The synaptic current decay depends mainly on the slowest component (τ_4) of the distribution (Wyllie *et al.* 1998). For wild-type channels ($n = 5$, mean ± S.E.M.) $\tau_4 = 8.4 \pm 3.0$ ms, for ϵL78P channels ($n = 5$) $\tau_4 = 54.6 \pm 6.8$ ms. To determine the effect of the ϵL78P mutation, the rate constants in a scheme with two binding sites and singly liganded openings (Colquhoun & Sakmann, 1985) were estimated from single-channel data. The likelihood of the entire sequence of open and shut times was maximised with exact allowance for missed brief events (Colquhoun *et al.* 1996; HJCFIT program). With these methods the total dissociation rate, diliganded channel closing rate (α_2) and diliganded channel opening rate (β_2) can be measured accurately. For the wild-type channels ($n = 5$) total dissociation rate was $15700 \pm 887\ s^{-1}$, $\alpha_2 = 1540 \pm 148\ s^{-1}$ and $\beta_2 = 44900 \pm 5040\ s^{-1}$. For ϵL78P channels ($n = 5$) total dissociation rate was $4680 \pm 1120\ s^{-1}$, $\alpha_2 = 780 \pm 131\ s^{-1}$ and $\beta_2 = 63700 \pm 6870\ s^{-1}$. Thus the effect of the ϵL78P mutation is to slow dissociation of ACh 3.4-fold, and to decrease α_2. Combined with a slight increase in β_2 this results in a 2.8-fold increase in the efficacy, defined as β_2/α_2.

Colquhoun D & Sakmann B (1985). *J Physiol* **369**, 501–557.

Colquhoun D *et al.* (1996). *Phil Trans R Soc Lond* A **354**, 2555–2590.

Croxen R *et al.* (2002). *Neurology* **59**, 162–168.

Wyllie D *et al.* (1998). *J Physiol* **510**, 1–18.

This work was supported by the MRC and The Wellcome Trust.

C87

GABA release during simulated ischaemia of rat hippocampal slices

Nicola J. Allen, David J. Rossi* and David Attwell

*Department of Physiology, University College London, Gower Street, London WC1E 6BT, UK and *Neurological Sciences Institute, OHSU, 505 NW 185th Avenue, Beaverton, OR 97006-3499, USA*

During brain ischaemia a release of glutamate into the extracellular space, largely by reversal of uptake by glutamate transporters (Rossi *et al.* 2000) and independent of action potentials, triggers neuronal death. The rundown of ion gradients in ischaemia is also expected to reverse uptake by GABA transporters. GABA release and consequent $GABA_A$ receptor activation could be neuroprotective because of the hyperpolarization it may produce, but might contribute to neuronal death by activating a Cl^- influx which facilitates water influx and cell swelling.

We whole-cell clamped CA1 pyramidal cells at 32–34 °C in hippocampal slices of P12 rats (killed humanely according to Home Office regulations), simulated ischaemia chemically (Rossi *et al.* 2000), and used the cells' $GABA_A$ receptors to sense the extracellular GABA concentration. The intracellular solution had a chloride concentration giving $E_{Cl} = 0$ mV. As reported by Rossi *et al.* (2000), after 6–7 min ischaemia, a large inward current which decayed to a maintained plateau was recorded at −30 mV, which in part reflects glutamate release.

When using an internal solution providing slow calcium buffering (containing 5 mM EGTA and 0.5 mM $CaCl_2$), applying GABA (1 mM) or the $GABA_A$ receptor blocker GABAzine (10 μM) during the ischaemia-induced current plateau evoked no change in current, whereas with strong calcium buffering (10 mM BAPTA and 0 mM $CaCl_2$) GABA evoked an extra inward current and GABAzine suppressed approximately one-third of the plateau current. This suggests that with the EGTA-based internal solution the rise of $[Ca]_i$ occurring during ischaemia leads to desensitization of $GABA_A$ receptors (Stelzer & Shi, 1994; Harata *et al.* 1997), but when $[Ca]_i$ is kept low with the BAPTA-based internal the whole-cell clamped neuron can be used to sense ischaemia-evoked GABA release. With the BAPTA-based internal solution, the GABAzine-blocked current during the ischaemic plateau was not significantly affected by TTX (1 μM, $P = 0.47$ by 2-tailed t test, 6 cell pairs), but the presence of SKF-89976a (100 μM) to block the neuronal GABA transporter GAT-1 reduced the GABAzine-suppressed current by 70 % ($P = 0.0034$, 8 cell pairs).

These data suggest that there is a significant elevation of extracellular GABA concentration during ischaemia, and that much of the GABA release occurs by reversed uptake.

Harata N *et al.* (1997). *J Physiol* **500**, 673–688.

Rossi D *et al.* (2000). *Nature* **403**, 316–321.

Stelzer A & Shi H (1994). *Neuroscience* **62**, 813–828.

This work was supported by The Wellcome Trust, a Wolfson-Royal Society award, a Burroughs-Wellcome Fellowship (D.J.R.), and the 4 year PhD Programme in Neuroscience at UCL (N.J.A.).

All procedures accord with current UK legislation.

C88

Shunting inhibition and mGluR-mediated disinhibition modulate the gain of granule cell input–output relationships during synaptic excitation in rat cerebellum

Simon J. Mitchell and R. Angus Silver

Department of Physiology, University College London, Gower Street, London WC1E 6BT, UK

Shunting inhibition modulates the input resistance of neurons, reducing the slope of the relationship between subthreshold voltage and injected current. However, the effect of inhibition on firing rates is controversial since in some studies inhibition offsets the suprathreshold input–output (I-O) relationship, while in others it changes the gain. Inhibition in granule cells (GCs) is controlled by Golgi cell firing rate and by glutamate spillover, which activates presynaptic mGluRs on Golgi cells, suppressing inhibition (Mitchell & Silver, 2000). We have investigated the modulation of GC I-O relationships by inhibition and presynaptic mGluRs.

Parasagittal slices of cerebellum (250 μm) were prepared from 25-day-old Sprague-Dawley rats, killed by decapitation. Whole-cell current-clamp recordings were made from GCs at 37 °C from a holding potential of −75 mV. Data are presented as means ± S.E.M. The mechanisms underlying gain modulation were studied using a single compartment conductance-based integrate-and-fire (I&F) model.

When GCs were driven by injected synaptic conductance waveforms, tonic inhibition reduced the gain of I-O relationships by 44 ± 6 % ($n = 5$) and offset the relationship by 16 ± 3 Hz ($n = 5$). However, during tonic excitation, the gain was unaltered by tonic inhibition (−8 ± 4 %; $n = 6$), whereas the relationship was shifted to the right (400 ± 50 pS; $n = 6$). These results show that tonic inhibition modulates the GC I-O relationship in different ways depending on whether excitation is synaptic or tonic.

Speeding the synaptic decay time constant and reducing the number of excitatory inputs, which both increase the coefficient of variation of the excitation train, increased gain changes in the I&F model. This suggests that the level of fluctuations in the excitatory waveform determines inhibition-mediated gain modulation.

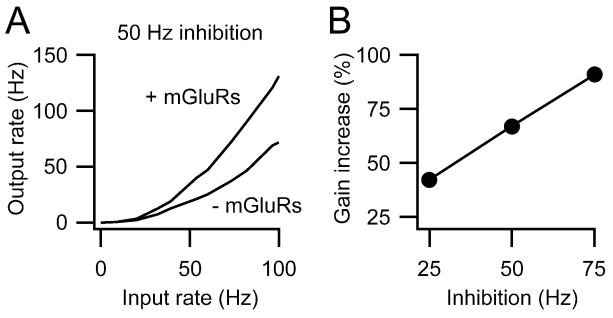

Figure 1. mGluR-mediated suppression of inhibition increases neuronal gain. A, synaptic I-O relationships for I&F model during 50 Hz inhibition, with and without the inclusion of mGluRs. B, increase in synaptic I-O relationship gain by mGluRs as a function of inhibition rate.

Having shown that inhibition can reduce GC gain, we studied how suppression of inhibition by mGluRs affects the GC I-O relationship. Inclusion of mGluRs in the model increased the gain of synaptic I-O relationships during inhibition (Fig. 1A). The fractional increase in gain produced by mGluRs increased as a function of inhibition (Fig. 1B).

Our results suggest that inhibition and mGluR-mediated disinhibition can act as cellular mechanisms for gain control in granule cells.

Mitchell SJ & Silver RA (2000). *Nature* **404**, 498–502.

This work was funded by The Wellcome Trust and the EC. R.A.S. is in receipt of a Wellcome Trust Senior Fellowship.

All procedures accord with current UK legislation.

C89

$GABA_A$ receptor-mediated tonic conductance differs between interneurons and pyramidal neurons in the hippocampus

M.C. Walker, D.M. Kullmann and A. Semyanov

Institute of Neurology, University College London, Queen Square, London WC1N 3BG, UK

$GABA_A$ receptors modulate the excitability of neurons by mediating IPSCs, but have also been shown to mediate a tonic current in cerebellar and hippocampal granule cells. We have recently reported that synaptic $GABA_A$ receptors in interneurons and pyramidal cells of the CA1 region of the hippocampus show several pharmacological and biophysical differences (Semyanov & Kullmann, 2002). Here we report that GABA receptor-mediated tonic conductance also differs between the two cell types.

We obtained hippocampal slices from guinea-pigs killed by cervical dislocation. Whole-cell recordings were made either from interneurons (stratum radiatum or oriens) or from pyramidal cells in CA1. Spontaneous IPSCs (sIPSCs) were isolated by applying ionotropic glutamate and $GABA_B$ receptor blockers. Because the pipette solution contained a high Cl^- concentration, both tonic and phasic $GABA_A$ receptor-mediated currents were inward.

Perfusion of the broad spectrum $GABA_A$ receptor antagonist picrotoxin (100 μM) abolished sIPSCs in both interneurons ($n = 7$) and pyramidal cells ($n = 6$). It also reduced the holding current in interneurons but not pyramidal cells, implying that a tonic conductance is only present in interneurons. Similar results were obtained with the $GABA_A$ receptor antagonist bicuculline (10 μM, $n = 4$). Surprisingly, the holding current in interneurons was unaffected by 0.5 μM gabazine, even though this completely abolished sIPSCs ($n = 6$). Increasing the extracellular GABA concentration with the GABA transport inhibitor NO711 (20 μM), caused an increase in the $GABA_A$ receptor-mediated tonic current in interneurons and also led to the appearance of a tonic current in pyramidal cells. This result suggests that differences in GABA transport may account for cell-type differences in tonic inhibition in the hippocampus.

Blockade of the tonic $GABA_A$ receptor-mediated conductance led to an increased excitability of interneurons in response to current injection. This also resulted in an increased frequency of sIPSCs in pyramidal neurons.

The greater expression of tonic inhibition in interneurons may reflect a homeostatic role for this phenomenon: increases in extracellular GABA may render GABAergic cells relatively

inexcitable, and therefore lead to a decrease in GABA release. This phenomenon may play an important role in regulating the excitability of the hippocampus.

Semyanov A & Kullmann DM (2002). *Neuropharmacology* **43**, 726–736.

All procedures accord with current UK legislation.

C90

α7-Nicotinic receptor-mediated modulation of GABAergic signalling in the hippocampus

A. Semyanov, M.C. Walker, N. Wanaverbecq and D.M. Kullmann

Institute of Neurology, University College London, Queen Square, London WC1N 3BG, UK

GABAergic transmission in the hippocampus can be modulated by several presynaptic heteroreceptors, including mGlu, $GABA_B$ and kainate receptors, which detect transmitter release from intrinsic neurons. However, the hippocampus also receives afferents from other structures, which may also influence synaptic transmission via heteroreceptors. Here we report that α7-nicotinic receptors (nAChRs) can modulate $GABA_A$ receptor-mediated signalling in the rodent hippocampus.

We obtained hippocampal slices from guinea-pigs killed by cervical dislocation. CA1 pyramidal cells and stratum radiatum interneurons were recorded in whole-cell voltage-clamp mode in the presence of antagonists of AMPA, kainate, NMDA, group III mGlu and $GABA_B$ receptors. Stimuli were delivered to stratum radiatum to isolate $GABA_A$ receptor-mediated IPSCs.

Application of the α7-nAChR agonist choline (1 mM) produced a reversible depression of the IPSC amplitude to 78 ± 2% (mean ± S.E.M., $P < 0.01$, paired t test, $n = 5$) and 84 ± 3% ($P < 0.01$, $n = 6$) of baseline in interneurons and pyramidal cells, respectively. Similar results were obtained with another α7-nAChR agonist, 4OH-GTS-21 (3 μM). In order to test whether endogenous ACh, released from cholinergic afferent fibres, could reproduce these effects, we delivered tetanic stimuli (20 pulses, 100 Hz) to stratum oriens. This resulted in a long-lasting (10 min) depression of the evoked IPSCs (86 ± 4% of baseline: $P < 0.01$; $n = 8$). We confirmed that this effect was mediated by acetylcholine release acting on α7-nAChRs by demonstrating that it could be potentiated by application of the acetylcholine cholinesterase inhibitor eserine ($n = 8$), and abolished by the α7-nAChR antagonist methyllycaconitine ($n = 8$).

ACh-mediated depression of IPSCs in CA1 neurons provides a powerful method of modulating hippocampal excitability and may contribute to cholinergic effects on learning and memory.

We are grateful to Dr R.L. Papke for the gift of 4OH-GTS-21.

All procedures accord with current UK legislation.

C91

Human recombinant neuronal nicotinic receptors: expression of tandem subunit constructs

Steven Broadbent, J.P. Boorman, P. Groot-Kormelink and L.G. Sivilotti

Pharmacology, The School of Pharmacy, 29/39 Brunswick Square, London WC1N 1AX, UK

Neuronal nicotinic acetylcholine receptors are pentameric ligand-gated ion channels. The large number of different subunits that can be expressed *in vivo* makes it difficult to know the exact make-up of the receptors present in neurones. As native receptors can contain more than two different subunits, it is important to be able to express homogeneous populations of such receptors heterologously. In order to restrict the stoichiometry of recombinant nAChRs, tandem constructs were created by linking α3 and β4 subunits and were expressed in *Xenopus* oocytes along with different monomer subunits. Oocytes were then tested with acetylcholine, using two-electrode voltage clamp, to see which tandem/monomer combinations produced functional receptors.

Tandems of the α3-β4 orientation failed to produce functional receptors either when expressed alone or along with any monomer. Tandems of the β4-α3 orientation did not produce functional receptors when expressed alone or along with α3, α4, α6 or β3 subunits (small responses were observed with monomer α2, α5 or β2 subunits). When the β4-α3 tandem was expressed along with β4 subunits, large inward currents were observed in response to acetylcholine. Dose–response curves were therefore obtained for β4-α3 + β4 receptors ($n = 4$) and compared with those from α3β4 receptors expressed from monomeric constructs ($n = 10$). The tandem-containing receptors were found to be macroscopically indistinguishable from α3β4 receptors ($EC_{50} = 122 \pm 8$ *vs.* 134 ± 6 μM; $n_H = 1.98 \pm 0.21$ *vs.* 1.73 ± 0.11, means ± S.D.).

We next wanted to check that receptors expressed from β4-α3 with β4 did actually contain two copies each of the α and β subunits from the tandem construct and one copy of the subunit from the β monomer cRNA. This was done by mutating from leucine to threonine the 9′ residue in the pore-lining region of the β subunit contained in the tandem construct. In channels of the nicotinic superfamily, incorporation of this mutation increases the receptor agonist sensitivity by an amount that is roughly proportional to the number of mutation copies present. Expressing β4-α3 + $β4^{LT}$ should give rise to a homogeneous population of receptors with a dose–response curved shifted to the left because of the presence of a single copy of the mutation. Nevertheless, dose–response curves obtained from such mutant combinations typically showed more than one component, indicating the simultaneous presence in the receptor population of channels containing different numbers of mutation copies and therefore different numbers of β subunit produced by the monomer cRNA.

These results indicate that caution has to be exercised in the interpretation of data from the expression of tandem constructs of nicotinic subunits.

This work was supported by the MRC, The Wellcome Trust (project grant 064652) and the School of Pharmacy.

All procedures accord with current UK legislation.

C92

α-Conotoxins PnIA and [A10L]PnIA stabilise different states of the α7 neuronal nicotinic acetylcholine receptor

R.C. Hogg*†, D.J. Adams*, P.F. Alewood* and D.C. Bertrand†

School of Biomedical Sciences, University of Queensland, Brisbane, Australia and †Department of Physiology, CMU, Geneva, Switzerland

The α-conotoxins are selective inhibitors of nicotinic acetylcholine receptors (nAChRs). An α-conotoxin, PnIA, isolated from *Conus pennaceus* has been demonstrated to be an inhibitor of native nAChRs in dissociated neurones and recombinant nAChRs, with a poor selectivity between receptor subtypes. Substitution of a leucine for alanine at position 10 renders the toxin a selective inhibitor of the α7 nAChR subtype (Hogg *et al.* 1999; Luo *et al.* 1999). It is assumed that PnIA and [A10L]PnIA inhibit the α7 nAChR by stabilising the receptor in a non-conducting desensitised or resting state. To determine which state these compounds stabilise and which amino acid residues are involved, the effects of PnIA, [A10L]PnIA and alanine scan mutants of [A10L]PnIA were investigated in homomeric chick α7 nAChRs and α7 receptors with the L247T mutation expressed in *Xenopus* oocytes. The α7L247T mutation causes the desensitised state of the receptor to become conducting (Bertrand *et al.* 1997). Use of the desensitized open α7L247T mutant allows us to probe the toxin effects on an otherwise electrophysiologically silent state of the receptor.

PnIA completely inhibited the ACh-evoked current in wild-type α7 receptors and α7L247T receptors with IC_{50} values of 349 and 194 nM, respectively. [A10L]PnIA and the [A10L]PnIA alanine mutants inhibited ACh-evoked currents in wild-type α7 nAChRs with an IC_{50} of 168 nM. In contrast, when co-applied with ACh, [A10L]PnIA and the alanine mutants potentiated the ACh-induced responses at α7L247T receptors and in addition [A10L]PnIA activated a current at α7L247T receptors in the absence of ACh. This illustrates that PnIA and [A10L]PnIA inhibit α7 receptors by stabilising different states of the receptor. PnIA stabilises a state which is non-conducting in both the wild-type and αL247T receptors that might correspond to the resting state, whereas [A10L]PnIA is supposed to stabilise the desensitised state which is closed in the wild-type and conducting in the αL247T receptor. These data illustrate that the presence of the longer aliphatic side chain at position 10 is sufficient to change the selectivity of the toxin for different states of the receptor.

Bertrand S *et al.* (1997). *NeuroReport* **8**, 3591–3596.

Hogg RC *et al.* (1999). *J Biol Chem* **274**, 36559–36564.

Luo S *et al.* (1999). *Biochemistry* **38**, 14542–14548.

All procedures accord with current National guidelines.

C94

Ryanodine-sensitive calcium stores modulate the cholinergic response of cochlear hair cells

M. Lioudyno, E. Glowatzki, S. Parameshwaran-Iyer and P.A. Fuchs

The Center for Hearing and Balance, Department of Otolaryngology-HNS, Johns Hopkins University School of Medicine, Baltimore, MD 21205, USA

Efferent neurons from the superior olivary complex release ACh to hyperpolarize outer hair cells (OHCs) in the mammalian cochlea. OHC hyperpolarization results from the opening of calcium-dependent (SK) potassium channels, triggered by calcium influx through nicotinic cholinergic receptors. Within the hair cell an endoplasmic reticulum that is found in close apposition to the efferent contact has been proposed to serve as a synaptic calcium store. For example, perfusion of ryanodine into perilymph enhanced the potency of efferent inhibition (Sridhar *et al.* 1997), and OHCs isolated from the guinea-pig showed some sensitivity to ryanodine and caffeine (Evans *et al.* 2000). Here we examine the effect of compounds acting on ryanodine-sensitive stores for their ability to modulate the cholinergic response of OHCs in an organ of Corti preparation excised from the rat cochlea.

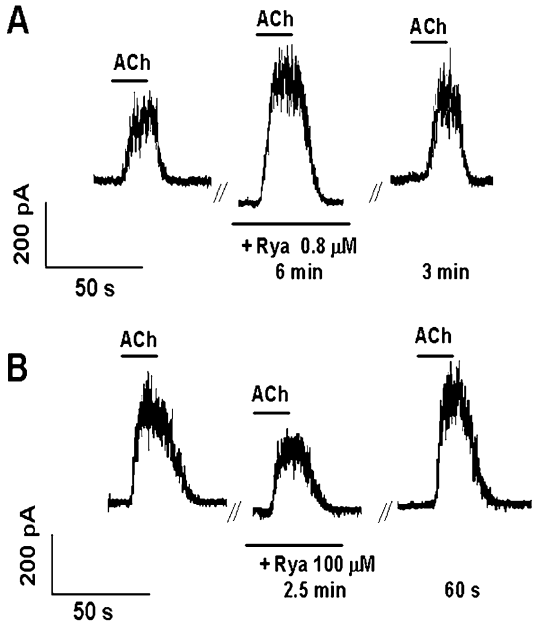

Figure 1. The effect of ryanodine (A: 0.8 μM, B: 100 μM) on the current at −30 mV evoked in OHCs by 100 μM ACh applied for 20 s. The time since application or removal of ryanodine is shown.

Rat pups (3–4 weeks old) were anaesthetized with pentobarbitone and decapitated as approved by the Animal Care and Use Committee. An apical turn of the organ of Corti was removed to a recording chamber on the stage of a compound microscope. Patch pipettes were used for whole-cell recordings from hair cells as described previously (Glowatzki & Fuchs, 1999). ACh alone or in combination with test compounds was applied from a perfusion array. Membrane potential of the OHC was held at −30 mV in most instances. The response to ACh consisted of an outward current up to 600 pA in amplitude. The average value was well maintained during a 20 s application of ACh, although the current fluctuated markedly about that mean. When ACh was applied in the presence of 0.5–1.0 μM ryanodine

the evoked current was 60 ± 29 % (S.E.M.) larger in six OHCs. When 100 μM ryanodine was applied the current evoked by ACh was reduced by 39 ± 4 % (6 cells). Application of 1 mM caffeine caused an initial augmentation of 14 ± 4 % (3 cells), followed within 8 min by inhibition (65 ± 6 %) of the ACh-evoked current (4 cells). These results demonstrate a consistent picture of sensitivity to compounds that act on calcium-induced calcium release via ryanodine receptors, supporting this mechanism as a contributory factor in the hair cell's cholinergic response.

Evans MG *et al.* (2000). *Cell Calcium* **28**, 195–203.
Glowatzki E & Fuchs PA (1999). *Science* **288**, 2366–2368.
Sridhar T *et al.* (1997). *J Neurosci* **17**, 428–437.

This work was supported by NIDCD DC01508.

All procedures accord with current National guidelines.

C95

The effect of light on calcium and light-induced calcium release in rods isolated from the salamander retina

Hugh R. Matthews* and Gordon L. Fain†

**Physiological Laboratory, University of Cambridge, Downing Street, Cambridge CB2 3EG, UK and †Departments of Physiological Science and Ophthalmology, UCLA, LA, CA, USA*

In darkness, Ca^{2+} enters through cGMP-gated channels in the rod outer segment and exits via Na^+/Ca^{2+}–K^+ exchange. Light closes the channels and decreases Ca_i^{2+}, but the relationship between light, current, and Ca_i^{2+} has remained unclear. We have previously shown that intense light evokes a release of Ca^{2+} within the outer segment (Matthews & Fain, 2001, 2002), most clearly seen when a rod is superfused with a $0Ca^{2+}/0Na^+$ solution designed to oppose surface membrane Ca^{2+} fluxes (Matthews *et al.* 1988; Nakatani & Yau, 1988). It seemed possible that this release would contribute to changes in Ca_i^{2+}. Using fluo-5F, rapid solution exchange, and suction pipette recording from rods isolated from salamanders killed humanely by stunning, decapitation and pithing, we now show that after saturating light the circulating current, Ca_i^{2+} and the light-releasable pool of Ca^{2+} all recover with a nearly identical exponential time course. Steady background light produces a maintained decrease in current, which is accompanied by a near-proportional decrease both in Ca_i^{2+} and in the light-releasable Ca^{2+} pool. These experiments show that the major determinant of Ca_i^{2+} in the outer segment following just-saturating illumination is the rate of influx through the channels, and that the light-releasable pool makes only a minor contribution. The amount of Ca in the light-releasable pool appears to be determined principally by Ca_i^{2+} except during bright light exposure. This is most clearly seen if the rod is illuminated in $0Ca^{2+}/0Na^+$ solution, since even relatively small bleaches in this solution deplete the pool even in the absence of a light-induced decline in Ca_i^{2+}, indicating some special effect of pigment bleaching on Ca^{2+} buffering and/or sequestration. This effect is spatially localised, since exposure to a narrow slit of intense light in $0Ca^{2+}/0Na^+$ solution eliminates the releasable pool in that location (after laser bleach fluo-5F fluorescence 0.99 ± 0.01 of initial dark level, mean ± S.E.M., 7 cells) but not in neighbouring unilluminated regions of the outer segment (after laser bleach fluo-5F fluorescence 1.23 ± 0.03 of initial dark level, 7 cells, significant at 0.1 % level, Student's unpaired *t* test, $t = 8.7$).

Matthews HR *et al.* (1988). *Nature* **334**, 67–69.
Matthews HR & Fain GL (2001). *J Physiol* **532**, 305–321.
Matthews HR & Fain GL (2002). *J Physiol* **542**, 829–841.
Nakatani K & Yau K-W (1988). *Nature* **334**, 69–71.

All procedures accord with current UK legislation.

C97

Characterisation of spontaneous intracellular Ca^{2+} transients in astrocytes from acute hippocampal rat slices

Susan J. Robertson

Academic Neurosurgery, King's College London, London SE5 9PJ, UK

Many recent studies on bi-directional communication between astrocytes and neurones suggest astrocytes have a form of excitability based on intracellular Ca^{2+} fluctuations. This study investigates the spontaneous Ca^{2+} fluctuations in astrocytes from the stratum radiatum. Wistar rats (P8–16) were killed by a Home Office approved humane procedure and brain slices prepared. Astrocytes were loaded with calcium green-1 AM (Kang & Nedergaard, 1999). Patch-clamp recording confirmed their identity as astrocytes (15/15 cells patched).

Astrocytes display spontaneous Ca^{2+} transients that persist in the absence of neuronal action potentials: control, 3.1 ± 0.7 mHz; 0.5 μM TTX, 4.4 ± 0.8 mHz ($n = 230$, 12 slices). Inhibition of the sarco(endo)plasmic reticulum Ca^{2+}-ATPases by cyclopiazonic acid (CPA, 50 μM) abolished the spontaneous calcium transients: control, 2.8 ± 0.4 mHz; CPA, 0.12 ± 0.05 mHz, $P < 0.001$; wash, 1.3 ± 0.3 mHz ($n = 101$, 5 slices), suggesting that the spontaneous transients are due to Ca^{2+} release from intracellular stores.

Inhibition of either Ca^{2+}-induced Ca^{2+} release (CICR) or IP_3-induced Ca^{2+} release with ryanodine (20 μM) or 2-APB (100 + 200 μM), respectively, did not inhibit the spontaneous transients. The involvement of nicotinic acid adenine dinucleotide phosphate has still to be investigated, thus the intracellular receptor mediating these events is still unknown. Many metabotrophic receptors signal via PLC, although the PLC inhibitor U73122 (10 μM) did not inhibit the spontaneous Ca^{2+} transients: control, 7.9 ± 1.0 mHz; U73122, 10.1 ± 1.9 mHz ($n = 161$, 6 slices).

Application of ATP or glutamate resulted in an increase in intracellular Ca^{2+}. In addition, ATP (100 μM) caused an increase in frequency of the spontaneous transients: TTX, 3.6 ± 0.7 mHz; TTX + ATP, 9.9 ± 2.2 mHz ($n = 171$, 8 slices, $P \leqslant 0.05$). In contrast, glutamate (100 μM) resulted in an initial increase in frequency followed by a significant reduction in the frequency of the transients during the glutamate-induced plateau. This persists for several minutes after glutamate washout and the resting Ca^{2+} had returned to control values: TTX, 2.1 ± 0.6 mHz; initial glutamate, 3.7 ± 0.7 mHz ($P \leqslant 0.05$); glutamate plateau, 1.0 ± 4.7 mHz ($P \leqslant 0.05$); wash, 1.9 ± 0.5 mHz ($n = 219$, 9 slices). Therefore it is likely that the spontaneous transients share a similar intracellular mechanism as the glutamate-induced rise in Ca^{2+} with ATP modifying the frequency of these transients. Values are means ± S.E.M.; significance levels were determined by Student's paired *t* tests or ANOVA.

Kang J & Nedergaard M (1999). Calcium imaging of identified astrocytes in hippocampal slices. In *Imaging Neurons: A Laboratory Manual,* ed. Yuste R, Lanni F & Konnerth A, pp. 42.1–42.11. Cold Spring Harbor Laboratory Press, New York.

This work was supported by TR Golden Charitable Trust, King's Medical Research Trust, HeadFirst, Patrick Berthoud Charitable Trust and Community Fund.

All procedures accord with current UK legislation.

C98

Glial glutamate transporters help to maintain independent operation of parallel fibre synapses in mouse cerebellar slices

Païkan Marcaggi, Daniela Billups and David Attwell

Department of Physiology, University College London, Gower Street, London WC1E 6BT, UK

There is controversy over the extent to which glutamate released at one synapse can diffuse to activate postsynaptic receptors at another nearby synapse. Uptake of glutamate helps to prevent such cross-talk, which could otherwise compromise the independence of signal transmission and information storage at individual synapses. We investigated the effect of preventing uptake by the glial transporters GLAST (knocked out in transgenic mice; Watase *et al.* 1998) and GLT-1 (blocked with 200 μM dihydrokainate), on parallel fibre EPSCs evoked at −70 mV in Purkinje cells from P14- to 21-day-old mice (killed humanely according to Home Office regulations).

If parallel fibre synapses operate independently then the EPSC waveform, and the effect on the waveform of blocking uptake, should be independent of the number of fibres stimulated. Experimentally, however, we found that when a single stimulus was applied in the molecular layer, the EPSC duration increased by 20 % as the number of fibres stimulated was increased from ~7 to ~90, and removal of GLAST (or block of GLT-1 when GLAST was knocked out) prolonged the EPSC much more when more fibres were stimulated. A similar effect of blocking GLT-1, dependent on the number of fibres stimulated, was seen both at 27 and at 36 °C. Thus there is cross-talk between parallel fibre synapses, even at a physiological temperature, and GLAST and GLT-1 curtail the EPSC by preventing glutamate diffusing between synapses.

When parallel fibre EPSCs were evoked by single stimuli to the granule cell layer, with the aim of producing a more physiological pattern of excitation (unlike for molecular layer stimulation which will activate many nearby fibres), the EPSC duration was shorter than for molecular layer stimulation, and was independent of the number of fibres stimulated, presumably because the activated fibres were separated by a distance too great for cross-talk to occur.

When trains of action potentials were evoked by molecular layer stimulation (200 Hz, 10 pulses), blocking uptake by GLAST (or blocking GLT-1 when GLAST was knocked out) dramatically prolonged the EPSC, even when only a small number of fibres were stimulated, presumably because the large amount of glutamate release saturated uptake by the remaining transporters present.

These results show that glial cell glutamate transporters increase the information processing capacity of the cerebellum by allowing neighbouring synapses to operate more independently.

Watase K *et al.* (1998). *Eur J Neurosci* **10**, 976–988.

We thank Professor K. Tanaka for the knock-out mice, and Stephen McGuiness for genotyping. This work was supported by a Marie-Curie Fellowship, the EU, The Wellcome Trust and a Wolfson-Royal Society Award.

All procedures accord with current UK legislation.

C99

Amyloid β peptide causes $[Ca^{2+}]_c$ fluctuations in rat astrocytes but not in hippocampal neurons in culture

Andrey Y. Abramov, Laura Canevari† and Michael R. Duchen

Department of Physiology, University College London, London WC1E 6BT and †Division of Neurochemistry, Institute of Neurology, London WC1N 3BG, UK

The deposition of amyloid β peptide (Aβ) in the CNS is a major feature of Alzheimer's disease. As Aβ peptides are toxic to neuronal cultures, we set out to explore of the underlying cellular processes that lead to toxicity. In the present series of experiments, we examined the action of Aβ on $[Ca^{2+}]_c$ homeostasis in cultures consisting of mixed glia and neurons or monocultures of astrocytes prepared from the hippocampi or cortices of neonatal rats which were humanely killed according to Home Office Guidelines (Vergun *et al.* 1999).

Cells were loaded with the $[Ca^{2+}]$ indicator fura-2 AM and images acquired using a cooled CCD camera. Aβ was applied either as the native peptide (amino acids 1–42) or as the 25–35 peptide fragment, while the reverse peptide fragment (35–25) served as a control. After a delay of ~5–10 min, both Aβ 25–35 and 1–42 (1–50 μM) increased $[Ca^{2+}]_c$ in cortical and hippocampal astrocytes in monoculture or in co-culture with neurons, but had no effect on $[Ca^{2+}]_c$ in neurons in the same experiments. The responses consisted of sporadic increases in $[Ca^{2+}]_c$ seen as either low amplitude (100–200 nM) $[Ca^{2+}]_c$ fluctuations or larger sustained increases in $[Ca^{2+}]_c$ (1–2 μM). The reverse peptide Aβ 35–25 had no effect. The Aβ-induced $[Ca^{2+}]_c$ signals persisted for hours after washout of Aβ. The $[Ca^{2+}]_c$ response to Aβ was entirely dependent on external calcium ($n = 231$), and neither U73122 (5 μM; $n = 89$), an inhibitor of PLC, nor 2-APB (40 μM; $n = 107$), an inhibitor of IP_3 Ca^{2+} channels, had any effect on the amplitude or shape of the $[Ca^{2+}]_c$ signals. Moreover, depletion of ER stores with the SERCA inhibitor thapsigargin did not prevent changes in $[Ca^{2+}]_c$ in response to Aβ ($n = 301$). The response was not affected by inhibitors of either ionotropic or metabotropic glutamate receptors, including CNQX, MK-801 or (S)MCPG ($n = 178$). However, responses were blocked by Zn^{2+} (1 mM, $n = 253$), which inhibits Aβ-induced pore formation (Lin *et al.* 2001) and by clioquinol (1 μM; $n = 207$), a chelator of heavy metal ions which prevents the formation of Aβ in complex with Cu^{2+} and Fe^{3+} (Cherny *et al.* 2001).

These data strongly suggest that Aβ causes $[Ca^{2+}]_c$ signals in astrocytes, but not in neurons, by insertion into the plasma membrane, where it forms a pore which opens sporadically. Such fluctuations of $[Ca^{2+}]_c$ over a long period of time may induce pathological changes in astrocytes and could be a trigger for neurotoxicity.

Cherny RA *et al.* (2001). *Neuron* **30**, 665–676.

Lin H *et al.* (2001). *FASEB J* **15**, 2433–2444.

Vergun O *et al.* (1999). *J Physiol* **519**, 451–466.

We thank The Wellcome Trust for support.

All procedures accord with current UK legislation.

C100

Characterisation of the calcium signals evoked by serotonin and ATP in rat sensory neurons

Alison F. Foster*, S. Bevan† and C.D. Richards*

**Department of Physiology, University College London, Gower Street, London WC1E 6BT and †Novartis Institute for Medical Sciences, 5 Gower Place, London WC1E 6BS, UK*

Sensory neurons can be activated by a variety of endogenous chemical mediators. Many of these mediators including ATP, serotonin (5-HT) and histamine are released from mast cells following an inflammatory stimulus. ATP and 5-HT are known pain-producing substances while histamine elicits either pain or itch, depending on the site of stimulation. While histamine has been shown to act via the H1 histamine receptor (Nicolson *et al.* 2002), the receptor subtypes responding to ATP and 5-HT remain unclear. Here we describe some experiments in which we have used calcium imaging to investigate the receptor subtypes involved in these responses.

Adult Wistar rats (200–250 g) were killed humanely by a rising CO_2 atmosphere. Sensory neurones were subsequently isolated from the dorsal root ganglion and maintained in Ham's F14 medium supplemented with nerve growth factor for 2–3 days as described previously (Bevan & Winter, 1995). The ratiometric dye fura-2 was used to estimate intracellular free calcium and the emitted fluorescence was collected with a cooled CCD system (see Nicolson *et al.* 2002). All experiments were performed at room temperature (21–25 °C).

In agreement with the data of Nicolson *et al.* (2002), the proportion of neurons responding to histamine with a rise in intracellular calcium was concentration dependent, with 32 % ($n = 74/233$) of neurons responding to 10 mM histamine. More than half of the sensory neurons (71 %, $n = 66/93$) responded to ATP (30 μM). The P_{2Y} agonist 2-methyl thio ATP also elicited responses in a significant proportion of the sensory neuron population (72 %, $n = 91/126$). The similarity of the time course and percentage of cells responding to ATP in 0 mM Ca^{2+} together with the activation of neurons by 2-methyl thio ATP suggests the involvement of a P_{2Y} receptor. Approximately a fifth (17 %, $n = 56/333$) of sensory neurons responded to 5-HT (100 μM). The percentage of cells that responded to 100 μM 5-HT in 0 mM Ca^{2+} (18 %, $n = 17/93$) is unchanged, implying that the 5-HT response is mediated via 5-HT_2 receptors.

In conclusion, it appears that the calcium responses elicited by 5-HT and ATP in rat sensory neurons are primarily due to activation of G protein-coupled receptors rather than ligand-activated ion channels.

Bevan S & Winter J (1995). *J Neurosci* **15**, 4918–4926.

Nicolson TN *et al.* (2002). *Neuroscience* **110**, 329–338.

A.F.F. is in receipt of a MRC collaborative studentship.

All procedures accord with current UK legislation.

C101

Mature nerve grafts rescue axotomised neonatal motoneurones from cell death

H.L. Low*, A. Nogradi†, G. Vrbova‡ and L. Greensmith*

**Sobell Department of Motor Neuroscience and Movement Disorders, Institute of Neurology, London, †University of Szeged, Hungary and ‡Department of Anatomy and Developmental Biology, University College London, London, UK*

Although peripheral nerve injury in neonatal rats is associated with poor axonal regeneration and extensive motoneurone death, the same injury in rats aged 5 days and older results in minimal motoneurone loss. It is known that mature nerves are better conduits for axon regeneration than immature ones. Here, we tested the possibility that the mature nerve micro-environment is also more conducive to motoneurone survival after injury. We also examined the role that integrins (extracellular matrix receptors) play in axon regeneration and motoneurone survival.

Three-day-old (P3) 'host' rats were anaesthetised with a 2 % halothane-oxygen mixture. The right sciatic nerve was transected and 5 mm nerve grafts from syngeneic 'donor' rats aged P3–P21 were attached to the cut ends of the host nerves. Seven days later, the host rats were terminally anaesthetised with phenobarbitone (100–200 mg, I.P.) and motoneurone survival was assessed. Nerve grafts were sectioned and stained for neurofilament and β-1 integrin immunoreactivity. In separate experiments, β-1 integrin function was blocked in P5 nerve grafts using a function-blocking antibody (monoclonal hamster anti-rat CD29, Pharmingen) and integrin expression was increased in P3 nerve grafts using a phorbol ester. Motoneurone survival and axonal regeneration was determined in both groups. All animal experiments conformed to Home Office Guidelines. Results were analysed using the Mann-Whitney *U* test for comparison of independent samples. Two-tailed tests were used in all instances, and the significance was set as $P < 0.05$.

Only 38.3 % (± 1.0 S.E.M., $n = 4$) of sciatic motoneurones in animals receiving P3 grafts survived. When nerve grafts from rats aged P5 were implanted, motoneurone survival rose to 71.4 % (± 3.2 S.E.M., $n = 5$). No further increase in motoneurone survival was observed with grafts from older donors. Blockade of β-1 integrins in P5 grafts reduced their survival-promoting effect and only 38.4 % (± 1.8 S.E.M., $n = 7$) of motoneurones survived. Increasing integrin expression in P3 grafts improves their ability to support motoneurone survival and 70.2 % (± 2.3 S.E.M.) of motoneurones survive. These changes in motoneurone survival were reflected in the extent of axon regeneration.

Thus the microenvironment that growth cones encounter during regeneration influences motoneurone survival. Implantation of mature nerve grafts can rescue motoneurones from cell death by a mechanism involving β-1 integrins.

The microenvironment that presents to regenerating growth cones greatly affects motoneurone survival and axon regeneration, with the 'mature' nerve microenvironment being more favourable. β-1 integrins appear to play a crucial role in this process.

This work was supported by the Brain Research Trust and The Wellcome Trust.

All procedures accord with current UK legislation.

C102

Caspase inhibitors rescue injured motoneurons

Dairin Kieran, Joanna Dekkers and Linda Greensmith

Sobell Department of Motor Neuroscience and Movement Disorders, Institute of Neurology, Queen Square, London WC1N 3BG, UK

Motoneurons are known to be vulnerable to the excitotoxic effects of glutamate, both *in vivo* and *in vitro*. Caspases have been shown to play a role in this glutamate-mediated death of motoneurons. Here, we examined the effect of treatment with caspase inhibitors on motoneuron survival both *in vitro*, following exposure to glutamate agonists, and *in vivo* following peripheral nerve injury.

All animal experiments were carried out humanely and conformed to Home Office Guidelines.

Primary motoneuron cultures were prepared from rat embryos of 14 days gestation. The donor animal was terminally anaesthetised with pentobarbitone (I.P., 140 mg kg^{-1}), and the embryos removed by hysterectomy, the ventral horns dissected and cultures prepared. At 7 days *in vitro* the cultures were exposed to AMPA (50 μM) for 48 h. To assess the effect of caspase inhibitors, in parallel cultures the caspase inhibitors BOC-D-FMK or QV-D-FMK (both 25 μM) were co-administered with the AMPA for 48 h. Motoneuron survival was assessed by counting the number of peripherin-positive neurons in each culture.

The effect of caspase inhibition was also assessed *in vivo*. The sciatic nerve was crushed in 3-day-old rats under halothane anaesthesia. At the same time, a 0.5 mg silicon implant containing either caspase inhibitor or sodium chloride was inserted under the meninges of the spinal cord between levels L1 and L5. Motoneuron survival was assessed 7 days after injury by counting the number of motoneurons in the operated and control ventral horns. The number of motoneurons on the operated side was expressed as a percentage of that on the contralateral control side of each animal.

Following treatment with 50 μM AMPA for 48 h *in vitro*, 47.4 % (± 3.9 S.E.M., $n = 5$) of motoneurons survive. When AMPA is co-administered with BOC-D-FMK or QV-D-FMK, motoneuron survival is increased to 82.9 % (± 4.2 S.E.M., $n = 5$) and 77.8 % (± 5.5 S.E.M., $n = 5$), respectively.

In vivo, 7 days after nerve crush only 58.2 % (± 2.4 S.E.M., $n = 3$) of motoneurons in the sciatic motor pool survive. Treatment with BOC-D-FMK improved motoneuron survival so that 73.1 % (± 4.8 S.E.M., $n = 3$) of motoneurons survive.

Thus treatment with either BOC-D-FMK or QV-D-FMK delays motoneuron cell death, both in *in vivo* and *in vitro* models of motoneuron degeneration.

This work was supported by the Brain Research Trust.

All procedures accord with current UK legislation.

C103

Treatment with hsp27 protects injured motoneurons from cell death induced by apoptotic stimuli *in vitro*

B. Kalmar, J. Dekkers, G. Burnstock and L. Greensmith

**Institute of Neurology and †Autonomic Neuroscience Institute, University College London, London, UK*

There is an increasing body of evidence that hsp27 protects cells against various insults. In addition, hsp27 has been found to interfere with the apoptotic cascade. We have recently shown that hsp27 expression is increased in motoneurons following neonatal nerve injury (Kalmar *et al.* 2002). Moreover, those motoneurons that survive injury and express hsp27 do not co-express markers of apoptosis such as activated caspase-3 (Kalmar *et al.* 2002). These results suggest that increased hsp27 expression may protect injured motoneurons from cell death. In this study we examined the effect of exogenous application of hsp27 protein on cell survival in an *in vitro* model of motoneuron degeneration.

Mixed cultures of ventral horn cells were prepared from E14 rat embryos (Camu & Henderson, 1994). All animals were humanely killed. At 7 days *in vitro* cells were exposed to stimuli that are known to induce apoptosis, such as staurosporin, H_2O_2 or the glutamate agonist AMPA, in the presence or absence of hsp27 (2 μg ml^{-1}; Stressgen). Control cultures were treated with vehicle (20 mM Tris pH 7.5, 10 mM NaCl, 1 mM EDTA, 1 mM DTT). Twenty-four hours later the cultures were stained with trypan blue in order to assess the extent of neuronal death. The cultures were then fixed and processed for peripherin immunocytochemistry. Peripherin is a specific marker of motoneurons in cultures of ventral horn cells. The effect of these treatments on motoneuron survival was assessed by counting the number of trypan blue-positive, peripherin-immunoreactive cells. Results are means ± S.E.M., and $n = 5$ in all cases. Significance was assessed by a Mann-Whitney U test and significance level was set at 0.05.

In untreated cultures only 5.1 ± 1 % of peripherin-positive cells were also positive for trypan blue. Treatment with apoptotic stimuli, however, resulted in an increase in motoneuron death, which is significantly reduced by co-treatment with hsp27. The results show that in staurosporin-treated cultures, 20.2 ± 4 % of motoneurons take up trypan blue compared with only 7.2 ± 2 % of those cultures co-treated with hsp27. Similarly, application of H_2O_2 onto motoneurons induces the uptake of trypan blue in 25.5 ± 5 % of motoneurons, which is significantly reduced in the presence of hsp27 to only 10.8 ± 3 %. Treatment with AMPA results in even more extensive motoneuron death, so that 31.7 ± 3 % of motoneurons are positive for trypan blue. In cultures co-treated with hsp27 and AMPA, motoneuron death was reduced to 14.8 ± 1.2 %.

These results show that manipulation of cellular hsp27 levels by exogenous application of hsp27 can rescue motoneurons from cell death induced by a variety of apoptotic stimuli.

Camu W & Henderson CE (1994). *J Neurol Sci* **124**, suppl., 73–74.

Kalmar B *et al.* (2002). *J Neurotrauma* **19**, 667–679.

This work was supported by the BRT.

All procedures accord with current UK legislation.

C103b

Depolarization-induced Ca^{2+} influx modulates glycinergic synaptic current in rat hypoglossal motoneurons

Davide Ragozzino*, Marat Mukhtarov† and Piotr Bregestovski†

**Dipartimento di Fisiologia Umana e Farmacologia, Università La Sapienza, Roma, Italy and †Institut de Neurobiologie de la Méditerranée (INMED), INSERM U29, Marseille, France*

Glycine receptors, mediating inhibition in spinal cord and brainstem, are modulated by intracellular Ca^{2+}, whose increase leads to the fast potentiation of glycine-activated currents (Fucile *et al.* 2000). To understand the physiological relevance of this Ca^{2+}-dependent modulation, we analysed the effects of intracellular Ca^{2+} increase on glycinergic synaptic currents. Patch-clamp recordings were performed from visually identified motoneurons of the hypoglossal nucleus in rat (P6–P9) brainstem acute slices (250 μm). The rats were humanely killed and all procedures complied with the guidelines of the French Animal Care Committee. In the presence of glutamatergic (CNQX, 10 μM, AP5, 40 μM) and GABAergic (bicuculline, 20 μM) blockers, stable strychnine-sensitive glycinergic synaptic currents were evoked by stimulation with an extracellular electrode close to the recorded neuron. To increase the cytosolic Ca^{2+}, the recorded neurons were repetitively depolarized from –100 to 0 mV (Lips & Keller, 1999). In the presence of a 'low Ca^{2+} buffer' concentration (0.5 mM BAPTA) the prolonged and repetitive depolarization of motoneurons (500 ms, 20 times, 1 Hz) induced: (1) a decrease in the amplitude (to 61 ± 4 %; mean ± S.E.M.) and (2) a prolongation in the decay kinetics (to 126 ± 9 %) of evoked glycinergic currents (Fig. 1*A, B* and *C*). Both effects were reversible; complete recovery was observed within a few minutes. In the presence of an antagonist of CB1 cannabinoid receptors (AM251, 0.5 μM) depolarization-induced depression of glycinergic currents was only to 80% of control, suggesting the involvement of CB1 receptors in the modulation of hypoglossal glycinergic synapses.

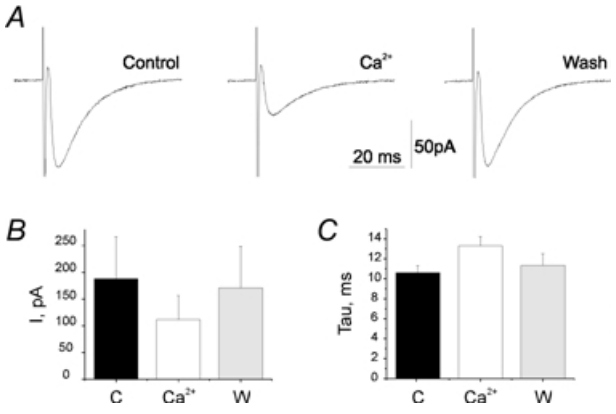

Figure 1. *A*, glycinergic synaptic currents recorded at –70 mV from a voltage-clamped hypoglossal motoneuron in a rat brainstem slice. Traces represent the average of 20 currents recorded before (left), immediately after (middle) and 3 min after (right) repetitive cell depolarization to 0 mV (500 ms, 1 Hz, 20 times). *B* and *C*, average peak amplitude (*B*) and decay time constant (*C*) of glycinergic synaptic currents recorded before (C), at 10–30 s (Ca^{2+}) and at 2–3 min (W) after repetitive depolarization.

Our results demonstrate the presence of a Ca^{2+}-dependent modulation of glycinergic synaptic transmission. Further studies have to be carried out for the characterization of the pre- and postsynaptic phenomena involved and to clarify the relationship between this form of modulation and previously described Ca^{2+}-dependent fast potentiation of glycine receptor currents.

Fucile S *et al.* (2000). *Neuron* **28**, 571.

Lips MB & Keller BU (1999). *J Neurophysiol* **82**, 2936.

All procedures accord with current National and local guidelines.

PC19

Upregulation of Na^+ pumping by glutamate in Purkinje cells isolated from rat cerebellar slices but not in glial cells isolated from salamander retinae

Jenny Pennack, Jaime McCutcheon and David Attwell

Department of Physiology, University College London, Gower Street, London WC1E 6BT, UK

Much of the energy used by the brain is expended on the Na^+/K^+ pump to restore ion gradients that are run down by neuronal activity (Attwell & Laughlin, 2001). When cells become highly loaded with Na^+ as a result of synaptic or action potentials, they may need to express more Na^+/K^+ pump subunits, or subunits of a lower Na^+ affinity, in order to maintain adequate transmembrane gradients of Na^+ and K^+. Exposure of cultured neurons and glia to glutamate has been shown to upregulate expression of Na^+ pump subunits (Brines & Robbins, 1993; Inoue *et al.* 1999).

We examined modulation of Na^+/K^+ pump activity in papain-isolated neurons (Purkinje cells from rat cerebellar slices; Billups & Attwell, 1996) and glia (Müller cells from *Ambystoma tigrinum* retinae; Brew & Attwell, 1987). (Animals were killed humanely in accordance with Home Office regulations.) After soaking in normal external (low K^+) solution containing either 200 μM or 0 μM glutamate, cells were whole-cell clamped with an internal solution containing 20 mM Na^+ (glia) or 60 mM Na^+ (neurons), in external solution containing 12 mM K^+, to activate the Na^+/K^+ pump. Strophanthidin (50 μM) was used to block the pump, generating an inward current proportional to the rate of pumping. Data were compared between cells by normalizing to cell capacitance, to compensate for differences in cell membrane area.

In salamander glia strophanthidin evoked an inward current of ~20 pA at −20 mV, which was larger at more positive potentials. Soaking in glutamate for 45 min, which will load the cells with Na^+ because of co-transport of 3 Na^+ with each glutamate anion by the glutamate transporters these cells express (Brew & Attwell, 1987), did not influence the size of the current (177 ± 20 pA nF^{-1} (mean ± S.E.M.) for 17 control cells, and 179 ± 15 pA nF^{-1} for 23 glutamate-soaked cells, $P = 0.95$ by two-tailed t test).

In Purkinje cells strophanthidin evoked an inward current of ~10 pA at 0 mV. Soaking in glutamate for 30 min, to Na^+-load the cells by activating AMPA receptors, increased the pump current by 53 %, from 253 ± 36 pA nF^{-1} in 14 control cells, to 385 ± 35 pA nF^{-1} in 15 glutamate-soaked cells ($P = 0.013$).

Further work is needed to ascertain the mechanism of the glutamate-evoked upregulation of neuronal pump rate, and to investigate why a similar upregulation is not seen in glia.

Attwell D & Laughlin SB (2001). *J Cereb Blood Flow Metab* **21**, 1133–1145.

Billups B & Attwell D (1996). *Nature* **379**, 171–174.

Brew H & Attwell D (1987). *Nature* **327**, 707–709.

Brines ML & Robbins RJ (1993). *Brain Res* **631**, 12–21.

Inoue N *et al.* (1999). *NeuroReport* **10**, 3289–3293.

This work was supported by The Wellcome Trust. Jenny Pennack is an M Biochem undergraduate at Bath University.

All procedures accord with current UK legislation.

PC20

Reactive oxygen species modulate neuronal excitability of rat intrinsic cardiac ganglia

K.A. Whyte, R.C. Hogg and D.J. Adams

School of Biomedical Sciences, University of Queensland, Brisbane, Queensland 4072, Australia

Reactive oxygen species (ROS) are produced as by-products of oxidative metabolism. ROS occur in the heart during ischaemia and coronary artery reperfusion, and have been implicated in cardiac dysfunction (Armour, 1999). The close proximity of the intracardiac ganglia (ICG) to the coronary blood supply makes them susceptible to the effects of ROS and it has been shown that hypoxia and post-ischaemic reperfusion influence the neuronal firing activity of ICG (Thompson *et al.* 1998). It is also known that ROS produced by the myocardium during ischaemia-reperfusion alters the firing properties of cardiac sensory neurites associated with afferent axons in vagal and sympathetic nerves (Huang *et al.* 1995; Ustinov & Schultz, 1994).

The present study investigated the effects of ROS upon the passive and active membrane properties, voltage-sensitive calcium channels (VSCC), and the delayed rectifier potassium channel in isolated neurones of rat neonatal (4–8 days old) and adult (> 6 weeks old; killed humanely in accordance with local guidelines) ICG using the dialysed whole-cell recording configuration of the patch-clamp technique. Bath application of ROS donors hydrogen peroxide (H_2O_2, 1 mM) and *tert*-butyl hydroperoxide (*t*-BHP, 1 mM) inhibited the depolarization-activated Ca^{2+} current and shifted the current–voltage (*I–V*) relationship to more hyperpolarized potentials in both neonatal and adult ICG. VSCC current amplitude in neonatal neurons were inhibited by H_2O_2 and *t*-BHP by 13.9 ± 2.6 % (mean ± S.E.M., $n = 8$) and 17.9 ± 1.9 % ($n = 5$), respectively, and by 7.8 ± 1.4 % ($n = 6$) and 16.5 ± 1.6 % ($n = 3$), respectively, in adult ICG neurones. In contrast, bath application of either H_2O_2 or *t*-BHP increased the amplitude of the delayed rectifier K^+ current by ⩾ 15 % ($n = 10$) in both neonatal and adult ICG neurones. Bath application of superoxide dismutase (SOD, 100 U ml^{-1}), a scavenger of ROS, to neonatal ICG also inhibited the VSSC current and shifted the *I–V* relationship to more depolarized potentials. Furthermore, in neonatal ICG, application of SOD prior to H_2O_2 or *t*-BHP attentuated the hyperpolarizing shift, but not the inhibition of VSCCs by H_2O_2 and *t*-BHP. In contrast, in adult ICG, application of SOD alone had no effect upon either VSCC current amplitude or *I–V* relationship, but application of SOD prior to H_2O_2 or *t*-BHP abolished the hyperpolarizing shift and inhibition by both ROS donors.

Under current-clamp conditions, H_2O_2 and *t*-BHP increased action potential duration by 16.2 ± 2.6 and 11.2 ± 2.8 % ($n = 4$), respectively, in neonatal ICG neurones and by 24.9 ± 2.8 and 24.1 ± 1.8 % ($n = 9$), respectively, in adult ICG neurones. Bath perfusion with either H_2O_2 or *t*-BHP reversibly hyperpolarized both neonatal and adult ICG neurones by > 5 mV ($n = 20$). Taken together, these data demonstrate that the effects of ROS alter depolarization-activated Ca^{2+} and K^+ conductances underlying neuronal excitability of ICG and therefore most likely modify autonomic control of the heart during ischaemia/reperfusion.

Armour JA (1999). *Cardiovasc Res* **41**, 41–54.

Huang HS *et al.* (1995). *Am J Physiol* **269**, H888–901.

Thompson GW *et al.* (1998). *Am J Physiol* **275**, H1434–1440.

Ustinov EE & Schultz HD (1994). *Circ Res* **74**, 895–903.

This research was supported by the NHMRC (Australia).

All procedures accord with current National and local guidelines.

PC21

Modulation by phosphorylation of the potassium channel KCNQ4 expressed in CHO cells

Jean-Marie Chambard, Rémi Louvel and Jonathan F. Ashmore

Department of Physiology and Centre for Auditory Research, University College London, Gower Street, London WC1E 6BT, UK

The voltage-gated potassium channel KCNQ4 is found by *in situ* hybridisation in outer hair cells of the mouse cochlea (Kubisch *et al.* 1999). It has been tentatively identified with a subunit of the hair cell potassium current, termed $I_{K,n}$, which is distinguished by an exceptionally negatively shifted activation curve ($V_{½}$ = −78 mV) (Kros & Marcotti, 1999). In contrast, KCNQ4 in oocytes activates slowly at more positive potentials ($V_{½}$ = −17.8 mV).

We used Chinese hamster ovary (CHO) cells as a mammalian expression system. The normal electrophysiological phenotype of these cells is a small leak conductance. To study the properties of KCNQ4, we have co-transfected CHO cells with the plasmids containing cDNAs of KCNQ4 (a gift from T.J. Jentsch) and green fluorescent protein (pEGFP-N1, Clonetech), both driven by a CMV promotor. Approximately 20 % of the cells were identified as showing GFP fluorescence. Of GFP-positive cells studied, over 80 % expressed a slowly developing outward current.

Using the whole-cell configuration of the patch-clamp technique, we have investigated the characteristics of these transfected cells. The average cell capacitance of the CHO cells was 22.2 ± 8.7 pF (mean ± S.D., $n = 21$). The outward current showed properties of KCNQ4. The current activated with a time constant of 110 ± 46 ms when the potential was stepped to 0 mV. At 0 mV the current was 2.64 ± 1.46 nA in amplitude. The current was half activated at a potential of −28.8 ± 8.0 mV. In eight cells, outward current was almost completely blocked by 200 μM linopirdine (mean inhibition 82 %). The anti-arrhythmic bepridil, a blocker of KCNQ1, applied at 10 μM, also blocked 49 % ($n = 3$) of the CHO outward currents.

Added to the bath, 500 μM 8-Br-cAMP activated outward current and shifted the $V_{½}$ by approximately 30 mV ($n = 5$). Added to the pipette solution, 50 U ml^{-1} of the β-catalytic subunit of PKA also induced a similar negative shift in two cells.

The most economical interpretation, consistent with the behaviour of adult hair cells, is that the potassium channel complex may be under the control of high levels of a cAMP protein kinase. Developing around postnatal day 10 in mouse such phosphorylation would produce the activation pattern of KCNQ4 and the negative resting potential found in adult hair cells.

Kros CJ & Marcotti W (1999). *J Physiol* **520**, 653–660.

Kubisch *et al.* (1999). *Cell* **96**, 437–446.

This work was supported by The Wellcome Trust.

PC22

Inputs to the suprachiasmatic nucleus from the intergeniculate leaflet and the optic nerve

J.A. Gonzalez and R.E.J. Dyball

Department of Anatomy, University of Cambridge, Cambridge CB2 3DY, UK

The suprachiasmatic nucleus (SCN) of the hypothalamus generates endogenous rhythms that control the daily cycles of many mammalian functions (Hastings & Maywood, 2000). The SCN needs to be entrained by external cues in order to adjust its activity to the environment. The cycles are entrained by both photic and non-photic cues. A number of inputs to the SCN have been described anatomically (Moga & Moore, 1997; Krout *et al.* 2002), amongst them inputs from the retina and from the intergeniculate leaflet (IGL) in the caudal thalamic region, deep to the lateral geniculate nucleus.

We attempted to characterise some of the connections using conventional extracellular recording techniques to monitor the response of single cells in the SCN following stimulation of the IGL area or the optic nerve (OptN). Recordings were made from single units in the SCN of urethane-anaesthetised (1.3 g kg^{-1} I.V.) male rats while stimulating the contralateral OptN exposed within the orbit. The effectiveness of stimulation of the optic nerve was confirmed by observing twitches in the rectus muscles of the eye. Another stimulating electrode was placed within the ipsilateral IGL area. The position of the electrodes was confirmed by histological reconstruction after the experiments. The responses of the SCN cells were assessed by creating peristimulus time histograms. All experiments were carried out in accordance with the Animals (Scientific Procedures) Act, 1986, and the rats were killed humanely at the end of the experiments.

Of a total of 85 SCN cells recorded, 20 (23.5 %) showed an excitatory response, 21 (24.7 %) an inhibitory response, and 11 (12.9 %) a complex response (with both excitatory and inhibitory components) after IGL stimulation. In contrast, only 14 (18.2 %) cells out of 77 showed a response to OptN stimulation. Of these, 10 (13 %) showed an excitatory response and 4 (5.2 %) were inhibited. In 8 of the 85 cells recorded no OptN response was tested. Whereas the responses seen after stimulating IGL were either long (> 20 ms; 40 out of 52, 77 %) or short ($\leqslant$ 20 ms; 12/52, 23 %) in latency, only long latency responses were seen after stimulating the OptN.

We conclude that there is a strong functional projection from the IGL to the SCN comprising both inhibitory and excitatory pathways. The different latencies of the responses suggest the existence of both monosynaptic and polysynaptic pathways. Since all the OptN responses were delayed, it seems probable that the projections to the SCN from OptN are polysynaptic and probably do not involve the IGL.

Hastings M & Maywood ES (2000). *Bioessays* **22**, 23–31.

Krout KE *et al.* (2002). *Neuroscience* **110**, 73–92.

Moga MM & Moore RY (1997). *J Comp Neurol* **389**, 508–534.

J.A.G. was supported by a Benefactors' Scholarship from St John's College, Cambridge.

All procedures accord with current UK legislation.

PC23

Prolonged glucose deprivation causes dramatic changes in $[Ca^{2+}]_i$ and mitochondrial responses to a toxic Glu challenge in young cerebellar granule cells (CGC)

Boris Khodorov*, Alexander Surin*, Alexey Bolshakov*, Maria Mikhailova*, Tatiana Storozhevykh†, Andryus Jurevicius†, Elena Sorokina†, Natalie Vinskaya† and Vsevolod Pinelis†

**Institute of General Pathology and Pathophysiology RAMS, 8 Baltiiskaya St., Moscow and †Scientific Center of Children's Health RAMS, 2/62 Lomonosovskii, Moscow, Russia*

Simultaneous measurements of $[Ca^{2+}]_i$ and mitochondrial potential (V_{mit}) were carried out in cultured rat CGC co-loaded with the low-affinity Ca^{2+} indicator fura-2FF and potentiometric probe rhodamine 123. Primary cultures of cerebellar granule cells (CGC) were prepared from Wistar rat pups aged 7–8 days (Khodorov *et al.* 1996). Animals were anaesthetized with ether and decapitated. The cells were plated onto poly-D-lysine-coated coverslips in MEM supplemented with 10% fetal bovine serum. In mature cells (15–17 DIV) a prolonged glutamate (100 μM Glu in Mg^{2+}-free, 10 μM glycine-containing medium) challenge induced a biphasic $[Ca^{2+}]_i$ increase associated with a profound mitochondrial depolarization (MD). Both these changes persisted in the post-glutamate period. In contrast in young cells (6–9 DIV) the same Glu application caused only small monophasic MD and a corresponding reversible $[Ca^{2+}]_i$ elevation. Earlier (Vergun *et al.* 1999) similar relationships were revealed in mature and young hippocampal neurones.

In the present study we found that the above difference between the effects of Glu on young and mature CGC can be eliminated by a prolonged replacement of glucose by its non-metabolised analogue 2-deoxyglucose (DOG, 10 mM) in all the external solutions. A continuous glucose deprivation induced the gradual MD which at the beginning could be abolished by oligomycin (2.5 μg ml^{-1}). Addition of Glu to the DOG-containing solution 20–90 min after the beginning of cell pretreatment induced a biphasic $[Ca^{2+}]_i$ increase associated with a MD which persisted during Glu washout even in the absence of Ca^{2+}in the medium.

This effect of glucose deprivation could not be prevented by L-NAME (the inhibitor of NO synthase) or MnTBAP (the scavenger of superoxide and/or hydrogen peroxide) but was greatly attenuated by addition of pyruvate (10 mM) to the DOG-containing medium.

Direct measurements of ATP content ([ATP]) performed in parallel experiments with sister CGC (employing luceferin-luceferase ATP assay) showed that pyruvate effectively diminished the DOG-induced decrease in [ATP] both at rest and during Glu application. This indicates that under conditions when glycolysis is suppressed the pyruvate-dependent respiration can maintain both high V_{mit} and [ATP] required by young neurons to withstand the toxic Glu challenge. The data suggest that a difference in the resistance of young and mature cultured cerebellar granule neurons to Glu is mainly determined by some peculiarities of their energetic metabolism.

Khodorov BI *et al.* (1996). *FEBS Lett* **393**, 135–138.

Vergun O *et al.* (1999). *J Physiol* **519**, 451–466.

This work was supported by The Physioogical Society UK, INTAS and RFBR.

All procedures accord with current National and local guidelines.

PC24

Dendritic properties of layer 2/3 neocortical pyramidal neurones studied *in vitro* and *in vivo*

Jack Waters, Matthew Larkum, Bert Sakmann and Fritjof Helmchen

Abteilung Zellphysiologie, Max-Planck-Institut für medizinische Forschung, D-69120 Heidelberg, Germany

Layer 2/3 (L2/3) and L5 pyramidal neurones receive ascending sensory input onto the basal and proximal regions of their dendritic arbours. The distal regions of the apical dendrites receive input from other sources, including projections from accessory sensory thalamic nuclei and from higher-order sensory regions. A cellular mechanism for associating these superficial- and deeper-layer inputs has been described in L5 neurones. This results from two cellular properties: active backpropagation of a somatically initiated action potential (AP) and a second AP initiation zone in the apical tuft. Here we consider whether L2/3 neurones have comparable dendritic properties. We studied L2/3 neurones in parasagittal slices (animals anaesthetised with halothane and decapitated) and in intact animals under urethane anaesthesia (2 g kg^{-1}; killed by cervical dislocation). We used whole-cell recording and calcium imaging to study apical dendrites of L2/3 pyramidal neurones in primary somatosensory cortex in acute slices (widefield imaging) and urethane-anaesthetized rats (intraperitoneal injection; imaging using 2-photon microscopy).

Both *in vitro* and *in vivo*, action potential (AP) amplitude declined gradually from the soma (to half the somatic amplitude at approximately 250 μm from the soma for deep layer 2/3 neurones *in vitro*). Calcium transients induced by single somatic APs were visible at (and often distal to) the principal bifurcation in all neurones, both *in vitro* and *in vivo*, but rarely in far distal L1 branches. Active AP backpropagation was confirmed *in vitro* by blocking sodium channels with TTX, which decreased both dendritic depolarization and the resulting calcium transient following injection of an AP-like waveform at the soma (under two-electrode voltage clamp).

L2/3 neurones also have a distal initiation zone since a dendritically initiated regenerative potential could be induced in the majority of neurones by dendritic current injection *in vitro*. A substantial dendritic calcium transient accompanied this dendritically initiated event. Pairing of a somatic action potential with subthreshold dendritic depolarization could also trigger a distal event. To date we have been unable to perform an equivalent experiment *in vivo*. However, a distal dendritic calcium transient of comparable amplitude to that observed during a dendritic event could be evoked by brief, high-frequency bursts of action potentials induced by somatic current injection. Burst-induced calcium transients were observed both *in vitro* and *in vivo,* indicating that dendritically initiated events may also occur *in vivo* in L2/3 pyramidal neurones.

These active dendritic properties provide a mechanism which enables L2/3 pyramidal neurones to act as cellular coincidence detectors that associate superficial- and deeper-layer inputs to the neocortex.

All procedures accord with current National and local guidelines.

PC25

Effect of inhibition of the F_1F_0- and the Na^+/K^+-ATPases on glutamate-induced changes in $[Ca^{2+}]_c$ and mitochondrial potential in rat hippocampal neurones in culture

Alexander Surin*, Boris Khodorov*, Tatiana Storozhevykh†, Vsevolod Pinelis† and Michael R. Duchen‡

**Institute of General Pathology and Pathophysiology RAMS, 8 Baltiiskaya St., Moscow, †Scientific Center of Children's Health RAMS, 2/62 Lomonosovskii, Moscow, Russia and ‡Department of Physiology, University College London, Gower Street, London, UK*

In hippocampal neurons in culture for > 11 DIV ('old neurons') exposure to glutamate (Glu) for 10–15 min causes in a profound increase in $[Ca^{2+}]_c$ and mitochondrial depolarisation (MD), which is sustained despite wash-out of Glu (Vergun *et al.* 1999). The objective of the present work was to test the hypothesis that this post-glutamate $[Ca^{2+}]_i$ plateau results from blockade of mitochondrial Ca^{2+} uptake combined with the depletion of intracellular ATP.

Primary cultures of hippocampal neurons were prepared from Wistar rat pups aged 1–2 days post-partum as described earlier (Vergun *et al.* 1999). Animals were anaesthetized with ether and decapitated. Rat hippocampal neurons in culture were co-loaded with the low affinity $[Ca^{2+}]$ indicator, fura-2FF-AM, and rhodamine 123 (Rh123) for simultaneous measurements of $[Ca^{2+}]_c$ and mitochondrial potential ($\Delta\Psi_m$), respectively. In old neurons, prolonged Glu challenge resulted in a biphasic $[Ca^{2+}]_c$ increase and a profound MD, which persisted after Glu wash-out. In contrast, in neurons at 6–8 DIV ('young neurons') a reversible monophasic $[Ca^{2+}]_c$ increase was associated with a very small MD.

Application of the protonophore FCCP (0.3 μM) to young neurones 3–5 min after the beginning of the exposure to Glu induced an additional profound MD and $[Ca^{2+}]_c$ elevation, which persisted despite Glu washout and only recovered after removal of FCCP. However, when oligomycin (2.5 μg ml^{-1}) or ouabain (0.5 mM) were applied prior to Glu exposure, then $[Ca^{2+}]_i$ decreased upon Glu withdrawal, despite the continuing FCCP-induced MD. Similar effects have been observed previously in cerebellar granule cells and may be explained if ATP required for operation of the plasmalemmal Ca^{2+} pump is depleted by ATP consumption by the reversed F_1F_0-ATP synthase (Khodorov, 2000) or by the Na^+/K^+-ATPase (Surin *et al.* 2000). In contrast, in old hippocampal neurones, treatment with either oligomycin or ouabain failed to prevent either MD or the $[Ca^{2+}]_c$ plateau in the post-glutamate period. These data suggest that the sustained $[Ca^{2+}]_c$ increase is not simply a consequence of the loss of $\Delta\Psi_m$ and ATP depletion and that some intrinsic mechanism that is specific to glutamate exposure inhibits the plasma membrane Ca^{2+}-ATPase and may be responsible for the failure of Ca^{2+} extrusion.

Khodorov BI (2000). *Membr Cell Biol* **14**, 149–162.

Surin A *et al.* (2000). *J Physiol* **528.P**, 69–70*P*.

Vergun O *et al.* (1999). *J Physiol* **519**, 451–466.

This work was supported by The Physiological Society UK, INTAS and RFBR grants.

All procedures accord with current UK legislation.

PC26

Involvement of c-Jun-N-terminal kinase (JNK) in β-amyloid-mediated impairment of long-term potentiation in the hippocampal CA1 *in vitro*

D.A. Costello and C.E. Herron

Department of Physiology, Conway Institute, University College Dublin, Dublin 2, Ireland

Alzheimer's disease is associated with elevated levels of β-amyloid (Aβ) peptide. Long-term potentiation (LTP) is an activity-dependent increase in synaptic efficacy, used as a cellular model of learning. Post-tetanic potentiation (PTP) is a short-term enhancement in synaptic transmission due to increased neurotransmitter release. A$\beta_{[25–35]}$ is known to depress LTP in the hippocampal CA1 region *in vitro* (Costello & Herron, 2002) while Aβ peptide also enhances the phosphorylation of JNK (Costello *et al.* 2002). We have investigated therefore the role of JNK in synaptic transmission and the Aβ-mediated depression of LTP. Experiments were performed on hippocampal slices (350 μm) from humanely decapitated male Wistar rats (50–100 g). Field excitatory postsynaptic potentials were recorded in the CA1 region and LTP was induced by trains of high-frequency stimuli (HFS) consisting of 10 trains of 10 pulses at 200 Hz (repeated three times at 20 s intervals) delivered to the Schaffer collateral/commissural pathway. In control slices, PTP recorded 5 min post-HFS measured 186 ± 7 % (EPSP slope ± S.E.M., $n = 8$) while robust LTP was recorded 60 min post-HFS (167 ± 5 %, $n = 8$). Application of A$\beta_{[25–35]}$ (200 nM) 60 min prior to HFS reduced significantly PTP and LTP (154 ± 8 %, $n = 6$, $P < 0.01$ and 137 ± 6 %, $n = 6$, $P < 0.005$, ANOVA). Application of SP600125, 30 min pre-HFS also impaired the level of LTP at concentrations of 1 or 20 μM (142 ± 7 %, $n = 5$, $P < 0.01$ and 142 ± 4 %, $n = 6$, $P < 0.005$, respectively) compared with controls. To investigate the effects of A$\beta_{[25–35]}$ when JNK was inhibited, SP600125 (1 and 20 μM) and A$\beta_{[25–35]}$ (200 nM) were applied 90 and 60 min, respectively, prior to HFS. Application of SP600125 prior to A$\beta_{[25–35]}$ did not alter significantly the impairment of LTP produced by either agent alone (133 ± 6 %; 1 μM SP600125+Aβ, $n = 5$ and 142 ± 6 %, 20 μM SP600125+Aβ, $n = 6$). Treatment with Aβ following prior application of 20 μM SP600125 reversed significantly the depression in PTP (186 ± 5 %, $n = 6$, $P < 0.005$) compared with Aβ alone. Baseline synaptic transmission was increased significantly following the application of 20 μM SP600125 (116 ± 4 %, $n = 6$, $P < 0.005$) accompanied by a reduction in paired pulse facilitation (inter-pulse interval 50 ms) (1.26 ± 0.06, $n = 6$, $P < 0.05$, unpaired t test) compared with controls (1.42 ± 0.03, $n = 6$). These results suggest that JNK is unlikely to be involved in the Aβ-mediated impairment of LTP. JNK may, however, play a direct role in neurotransmitter release and synaptic plasticity.

Costello DA & Herron CE (2002). *E J Physiol*. **433s**, 299*P*.

Costello D *et al.* (2002). *Proc FENS* 151.5.

This work was supported by the Health Research Board of Ireland and Enterprise Ireland.

All procedures accord with current National guidelines.

PC27

UTP and ATP evoke increases in intracellular Ca^{2+} via P2Y receptors in cultured chick utricular epithelia

E.O. Ako and J.E. Gale

Department of Physiology and Centre for Auditory Research, University College London, Gower Street, London WC1E 6BT, UK

Hair cells are the primary sensory receptors of the cochlea and vestibular systems. If hair cells are damaged or lost the surrounding support cells are triggered to divide to produce new hair cells. In some cases support cells are also thought to undergo phenotypic conversion to hair cells. Thus support cells are the progenitors of any newly replaced hair cells. Little is known about the physiology of vestibular support cells. We hypothesised that ATP might provide a trophic or mitogenic signal for support cells in damaged hair cell epithelia. Embryonic day 20 chicks were killed humanely, the utricles dissected out and treated with thermolysin to enable removal and culture of the epithelia sheet (Warchol, 2002). Cultures were loaded with fura-2 AM, and imaged during puff application of extracellular nucleotides at various concentrations. The UTP and ATP activated significant increases in the measured fura-2 ratio, proportional to increases in intracellular calcium ($[Ca^{2+}]_i$). Dose–response curves showed that the rank order for agonist potency was UTP > ATP >> UDP ~ ADP. The EC_{50} values for UTP and ATP were 0.5 ± 0.3 and 13.1 ± 2.5 μM, respectively (means ± S.D., $n \geqslant 3$ for each concentration). P2 receptors are classified into P2X and P2Y, the former being composed of ligand-gated ion channels and the latter being G-protein-coupled receptors (Ralevic & Burnstock, 1998). The increase in $[Ca^{2+}]_i$ we observe could therefore result from entry of calcium from the external medium via P2X receptors or release from intracellular stores activated via P2Y receptors. Pre-incubation with 1 μM thapsigargin prevented the changes in $[Ca^{2+}]_i$ activated by either UTP or ATP, suggesting P2Y receptor involvement. When both ATP and UTP were applied simultaneously at concentrations close to their EC_{50} values, the increase in $[Ca^{2+}]_i$ was not significantly different from the increase observed with applications of either nucleotide alone. The latter result suggests that the action of both UTP and ATP is via the same receptor(s). Application of 10 μM pyridoxal-phosphate-6-azophenyl-2′,4′-disolfonate (PPADS) significantly reduced the $[Ca^{2+}]_i$ rise to 25 % of control values evoked by UTP ($P < 0.05$, $n = 3$, Student's paired t test).

These results confirm the presence of P2Y receptors in support cells in chick utricular cultures. Given the profile we observe, we suggest that support cells express $P2Y_4$ and/or $P2Y_6$ receptors. The data also suggest a physiological role for signalling by extracellular nucleotides in the vestibular system.

Ralevic V & Burnstock G (1998). *Pharmacol Rev* **50**, 413–492.

Warchol ME (2002). *J Neurosci*. **22**, 2607–2616.

This work was supported by The Wellcome Trust, The Royal Society and a Physiological Society vacation studentship to E.O.A.

All procedures accord with current UK legislation.

PC28

TRPC3 channel-mediated capacitative calcium entry in cochlear outer hair cells

N.P. Raybould, D.J. Jagger, R. Kanjhan, D. Greenwood, P. Laslo, C. Soeller, M.B. Cannell and G.D. Housley

Department of Physiology, Faculty of Medicine and Health Sciences, University of Auckland, New Zealand

Cochlear outer hair cell (OHC) forward and reverse transduction is regulated by intracellular Ca^{2+} concentration ($[Ca^{2+}]_i$). Here we describe a capacitative calcium entry (CCE) mechanism in mammalian cochlear OHC. OHC were isolated from adult guinea-pigs and rats overdosed with pentobarbitone as previously described (Raybould *et al.* 1997). Using the whole-cell patch clamp technique, repeated voltage ramps were used to monitor membrane currents. In some experiments OHC $[Ca^{2+}]_i$ was measured using confocal microscopy. TRPC3 mRNA expression was assessed using RT-PCR analysis. Confocal immunofluorescence microscopy was used to localise TRPC3 protein in whole-mount rat and guinea-pig organ of Corti.

CCE was evident as a biphasic overshoot in OHC membrane current following transient lowering of $[Ca^{2+}]_i$. Application of the K_{Ca} channel blocker charybdotoxin (1 μM) almost completely blocked activation of the outward current and revealed a Ca^{2+}-permeable inward current. This inward current reversed at approximately +25 mV and was dependent on extracellular Ca^{2+} concentration with a threshold of approximately 600 μM.

The primary candidates for the ion channels that mediate CCE are the transient receptor potential (TRP) superfamily of proteins (Minke & Cook, 2002). External application of 2-aminoethyl diphenylborate (2APB, 250 μM–1 mM), an antagonist of TRPC3-mediated currents, produced a differential block of the inward component of the CCE-mediated overshoot in membrane current (Trebak *et al.* 2002). Inclusion of 2APB in the recording solution had no effect. Bath superfusion of 1-oleoyl-2-acetyl-sn-glycerol (OAG, a synthetic analogue of diacylglycerol; 100 μM–1 mM) produced an increase in membrane current consistent with PLC/DAG-mediated activation of TRPC subunit proteins (Hofman, 1999). These findings were confirmed by RT-PCR detection of TRPC3 mRNA and immunolocalisation of the TRPC3 protein in OHC to known regions of IP_3R expression (Mammano, 1999). CCE was not dependent on stored Ca^{2+}, as dumping of intracellular stores with the SERCA blocker cyclopiazonic acid (10 μM) had no effect on the CCE-mediated biphasic current response.

These findings suggest that OHC express TRPC3 subunit protein associated with a CCE pathway that provides a mechanism for the refilling of stores, and also complements Ca^{2+} signalling linked to IP_3R pathways activated by P2YR and AChR.

Hofmann T (1999). *Nature* **397**, 259–263.

Mammano F *et al.* (1999). *J Neurosci* **19**, 6918–6929.

Minke B & Cook B (2002). *Physiol Rev* **82**, 429–472.

Raybould NP *et al.* (1997). *J Physiol* **498**, 717–727.

Trebak M *et al.* (2002). *J Biol Chem* **277**, 21617–21623.

This work was funded by the Health Research Council, Marsden Fund and Deafness Research Foundation and approved by the University of Auckland Animal Ethics Committee.

All procedures accord with current National and local guidelines.

PC29

Regulation of cerebellar inhibitory synaptic plasticity by presynaptic NMDA receptors

I.C. Duguid and T.G. Smart

Department of Pharmacology, University College London, Gower Street, London WC1E 6BT, UK

Inhibitory synaptic transmission mediated by $GABA_A$ receptors on cerebellar Purkinje neurones (PNs) exhibits a long-lasting 'rebound potentiation' (RP) subsequent to repetitive hetero-synaptic climbing fibre activation (Kano *et al.* 1992). We report that during rebound potentiation a novel, enhancement in GABA release termed depolarization-induced potentiation of inhibition (DPI) that involves the retrograde release of a glutamate-like transmitter and subsequent activation of presynaptic *N*-methyl-D-aspartate (NMDA) receptors.

To induce DPI, cultured PNs (16–21 DIV) from Sprague-Dawley rats were voltage clamped at –70mV in normal ACSF containing both tetrodotoxin (TTX) and 6-cyano-7-nitroquinoxaline-2,3-dione (CNQX) to block action potentials and non-NMDA receptor-mediated currents. Cells were then subjected to a single depolarising pulse protocol that involved rapid depolarisation of the cell eight times from –70 to 0 mV (2 s intervals). RP (Llano *et al.* 1991; Kano *et al.* 1992) was associated with an increase in the mean mIPSC amplitude (146 ± 9 % of control; $n = 10$; $P < 0.01$; *t* test) while the mean mIPSC frequency displayed a clear biphasic profile. Initially, a rapid reduction in the mean mIPSC frequency was observed (79 ± 5% of control; lasting ~60 s), before developing into a novel, transient increase in the mean mIPSC frequency observed at 3 min post-stimulus (149 ± 8% of control; $n = 10$; $P < 0.01$). We examined whether the coincident presynaptic component to RP occurred also in immature (P6–8) slice preparations, during a stage in development when morphology and synaptic connectivity closely resembles that of cultured PNs. Induction of RP resulted in a similar increase in the mean mIPSC amplitude (154 ± 21% of control; $n = 7$; $P < 0.02$) and frequency (160 ± 30% of control; $n = 7$; $P < 0.02$) measured 5 min post-stimulus. The involvement of presynaptic NMDA receptors during the increase in GABA release was implicated by three main findings. Firstly, the antagonist, D-(2)-amino-5-phosphovalerate (D-APV; 50 μM), completely abolished the mIPSC frequency potentiation in both cultured and immature (P6–8) PNs (98 ± 11 % of control and 101 ± 13% of control, respectively). Secondly, brief (4 s), focal applications of NMDA (100 μM) induced a sustained increase in the release of GABA from basket/stellate cells persisting for > 13 min (no postsynaptic NMDA currents were observed). Finally, triple immunocolocalisation of NMDA receptor subunits (NR1, NR2A,C&D) provided further evidence for the existence of presynaptic NMDA receptors at putative basket/stellate cell axon terminals.

This presynaptic regulation of transmitter release, during the induction of cerebellar synaptic plasticity, will ensure control over PN excitability and subsequent sensorimotor co-ordination in the cerebellar cortex.

Kano M *et al.* (1992). *Nature* **365**, 601–604.

Llano I *et al.* (1991). *Neuron* **6**, 565–574.

This work was supported by the MRC.

All procedures accord with UK legislation.